Experimental Neurology xxx (xxxx) 114962

Contents lists available at ScienceDirect

Experimental Neurology

journal homepage: www.elsevier.com/locate/yexnr

Research paper

A comparison of the antiepileptogenic efficacy of two rationally chosen multitargeted drug combinations in a rat model of posttraumatic epilepsy

Mustafa Q. Hameed [a], Raimondo D'Ambrosio [b], Cliff Eastman [b], Benjamin Hui [a], Rui Lin [a], Sheryl Anne D. Vermudez [a], Amanda Liebhardt [a], Yongho Choe [a], Pavel Klein [c, d], Chris Rundfeldt [c], Wolfgang Löscher [c, e, 1, *], Alexander Rotenberg [a, c, 1, *]

[a] Department of Neurology and FM Kirby Neurobiology Center, Boston Children's Hospital, Harvard Medical School, Boston, MA, USA
[b] Department of Neurological Surgery, University of Washington, Seattle, WA, USA
[c] PrevEp, Inc., Bethesda, MD, USA
[d] Mid-Atlantic Epilepsy and Sleep Center, Bethesda, MD, USA
[e] Translational Neuropharmacology Lab, NIFE, Department of Experimental Otology of the ENT Clinics, Hannover Medical School, Hannover, Germany

ARTICLE INFO

Keywords:
Levetiracetam
Atorvastatin
Ceftriaxone
Kainate
Fluid percussion injury

ABSTRACT

Post-traumatic epilepsy (PTE) is a recurrent and often drug-refractory seizure disorder caused by traumatic brain injury (TBI). No single drug treatment prevents PTE, but preventive drug combinations that may prophylax against PTE have not been studied. Based on a systematic evaluation of rationally chosen drug combinations in the intrahippocampal kainate (IHK) mouse model of acquired epilepsy, we identified two multi-targeted drug cocktails that exert strong antiepileptogenic effects. The first, a combination of levetiracetam (LEV) and topiramate, only partially prevented spontaneous recurrent seizures in the model. We therefore added atorvastatin (ATV) to the therapeutic cocktail (TC) to increase efficacy, forming "TC-001". The second cocktail – a combination of LEV, ATV, and ceftriaxone, termed "TC-002" – completely prevented epilepsy in the mouse IHK model. In the present proof-of-concept study, we tested whether the two drug cocktails prevent epilepsy in a rat PTE model in which recurrent electrographic seizures develop after severe rostral parasagittal fluid percussion injury (FPI). Following FPI, rats were either treated over 3–4 weeks with vehicle or drug cocktails, starting either 1 or 4–6 h after the injury. Using mouse doses of TC-001 and TC-002, no significant antiepileptogenic effect was obtained in the rat PTE model. However, when using allometric scaling of drug doses to consider the differences in body surface area between mice and rats, PTE was prevented by TC-002. Furthermore, the latter drug cocktail partially prevented the loss of perilesional cortical parvalbumin-positive GABAergic interneurons. Plasma and brain drug analysis showed that these effects of TC-002 occurred at clinically relevant levels of the individual TC-002 drug components. In silico analysis of drug-drug brain protein interactions by the STITCH database indicated that TC-002 impacts a larger functional network of epilepsy-relevant brain proteins than each drug alone, providing a potential network pharmacology explanation for the observed antiepileptogenic and neuroprotective effects observed with this combination.

Abbreviations: ATV, atorvastatin; BBB, blood-brain barrier; BDNF, brain derived neurotrophic factor; CCI, controlled cortical impact; CTX, ceftriaxone; DAPI, 4′,6′-diamidino-2-phenylindole; *EAAT2, excitatory amino acid transporter 2*; *EEE*, recurrent epileptiform electrocorticographic event; ECoG, electrocorticography; EEG, electroencephalography; FPI, fluid percussion injury; GLT-1, glutamate transporter 1; HMGB1, h*igh mobility group box 1*; HMGCR, 3-hydroxy-3-methylglutaryl-CoA reductase; IHK, intrahippocampal kainate; IL-1β, interleukin 1β; LEV, levetiracetam; MCT, monocarboxylic acid transporter; MOA, mechanism of action; mTLE, mesial temporal lobe epilepsy; mTORC1, mechanistic target of rapamycin complex 1; OAT, organic anionic transporter; OATP, organic anion-transporting polypeptide; POC, proof-of-concept; PTE, post-traumatic epilepsy; PFA, paraformaldehyde; PNN, perineuronal net; PVI, parvalbumin-positive interneuron; SE, status epilepticus; STITCH, Search Tool for Interacting Chemicals; SV2A, synaptic vesicle glycoprotein 2 A; TBI, traumatic brain injury; TC, therapeutic cocktail; TPM, topiramate; WFA, *wisteria floribunda* agglutinin

* Corresponding authors at: PrevEp, Inc., Bethesda, MD, USA.
E-mail addresses: Loescher.Wolfgang@mh-hannover.de (W. Löscher), alexander.rotenberg@childrens.harvard.edu (A. Rotenberg).
[1] These authors share senior authorship

https://doi.org/10.1016/j.expneurol.2024.114962
Received 19 June 2024; Received in revised form 8 August 2024; Accepted 13 September 2024
0014-4886/

1. Introduction

Epilepsy is one of the most common neurological diseases, affecting about 70 million people worldwide (Devinsky et al., 2018). About 20 % of all epilepsies are acquired, either caused by traumatic brain injury (TBI), stroke, tumors, or infection (Klein and Tyrlikova, 2020). While these patients present to medical care at the time of the initial insult, TBI-induced primary and secondary structural and molecular brain alterations eventually lead to epilepsy, often after a latent period of weeks to months—a process termed epileptogenesis (Löscher, 2020; Dulla and Pitkänen, 2021). The latent period theoretically offers an opportunity to modify and prevent epileptogenesis, which remains the ultimate aim of clinical management and the 'holy grail' of drug development (Löscher, 2020; Koepp et al., 2024).

Over decades, the prevailing standard in drug discovery was the concept of designing highly selective compounds that act on individual drug targets (Hughes et al., 2011; Eder and Herrling, 2015; Deshaies, 2020). However, more recently, multi-target and combinatorial drug therapies have become an important treatment modality in complex diseases such as epilepsy (Deshaies, 2020; Löscher and Klein, 2022). The negative outcome of most single-drug epilepsy prevention trials in preclinical models or patients and the complexity of epileptogenesis led us to propose in 2013 that network or rational polypharmacy approaches may be more effective (Löscher et al., 2013). Based on this suggestion, we initiated a systematic approach to develop novel multi-targeted combinations of repurposed drugs for modification or prevention of epilepsy (Löscher and Klein, 2022). For this purpose, we have taken two strategies: (i) combining potentially synergistic drugs that have an antiepileptogenic or disease-modifying effect in an epilepsy model and have complementary mechanisms of action (MOAs), and (ii) a computational in silico approach for network analysis that allows to analyze the effects of these drug combinations on protein networks in the brain (Löscher and Klein, 2022).

Our initial effort to identify antiepileptogenic drug combinations yielded 12 lead multi-targeted combinations that we first examined for tolerability in mice and then evaluated for antiepileptogenic efficacy in the intrahippocampal kainate (IHK) mouse model of mesial temporal lobe epilepsy (mTLE), in which epilepsy develops after a kainate-induced status epilepticus (SE). Three effective and well-tolerated drug combinations were identified by these strategies (Löscher and Klein, 2022): a combination of levetiracetam (LEV) and topiramate (TPM) (Schidlitzki et al., 2020), a combination of LEV, TPM, and gabapentin, and a combination of LEV, atorvastatin (ATV) and ceftriaxone (CTX) (Welzel et al., 2021).

In humans, TBI is a much more common cause of acquired epilepsy than SE (Klein et al., 2018), so the demonstration of antiepileptogenic efficacy in a PTE model is important for the subsequent translation of effective drug combinations to clinical trials. We now report the next step of our systematic approach: evaluation of the most effective drug combinations in a second species, and in a second acquired epilepsy model, i.e., the fluid percussion model (FPI) of TBI-induced post-traumatic epilepsy (PTE) (Löscher and Klein, 2022).

Here, we summarize combining three distinct experiments to compare two drug combinations in the rat FPI PTE model: the therapeutic combination (TC) of LEV, TPM, and ATV (TC-001) and a combination of LEV, ATV, and CTX (TC-002). While this approach is unorthodox, these experiments are unified thematically and allow us to derive a single conclusion. The present study also provides data to inform the design of treatment protocols for future preclinical and clinical trials.

2. Materials and methods

2.1. Animals

Male rats were used for all experiments to eliminate the confounds of the estrous cycle. The experiments with TC-001 and the reduced dose of TC-002 were performed in Sprague-Dawley rats (P32–36) whereas the pilot experiment with a higher TC-002 dose was performed in Wistar rats (P56–63). Animals were housed 2–3 per standard cage until use and individually after the start of experimentation, in a specific-pathogen-free facility with ad libitum supply of food and water and a controlled 12-h light/dark cycle. The experiments on TC-001 were performed at the University of Washington (Seattle) while the experiments on TC-002 were performed at Boston Children's Hospital (Boston). Fig. 1 illustrates the protocol used for the experiments. All procedures were approved by the Institutional Animal Care and Use Committees at the University of Washington and Boston Children's Hospital, and in accordance with the National Institutes of Health Guide for the Care and Use of Laboratory Animals. All efforts were made to minimize animal pain and distress and numbers used.

2.2. Fluid percussion injury

Rostral parasagittal fluid percussion injury (FPI) was performed as detailed previously (Eastman et al., 2021; Hameed et al., 2023). Animals were anesthetized (induction: 4 % halothane/isoflurane; maintenance: 1–1.5 % halothane/isoflurane; in 30 % O2 and air), intubated, and mechanically ventilated. Animal temperature was maintained at 37 ˚C with a heating pad. For FPI, a 3–5 mm burr hole was drilled centered over the right (Seattle) or left (Boston) convexity equidistant between the lambda and bregma, with the lateral edge of the craniectomy adjacent to the lateral ridge of the skull. A female-to-female luer adapter (Cole-Palmer, Vernon Hills, IL) was secured to the surface of the skull over the craniectomy with cyanoacrylate adhesive and further secured with dental cement. Animals were disconnected from the ventilator, and a pressure pulse (8 ms, 3.5 atm) was delivered with the FPI device (Scientific Instruments, University of Washington; AmScien Instruments, VA; USA) and measured by a transducer (Entran EPN-D33-100P-IX, Measurement Specialties, Hampton, VA). Mechanical ventilation was resumed 10 s after injury to standardize post-traumatic apnea and hypoxia and terminated when spontaneous breathing resumed. Acute mortality rate due to FPI was ~25 %. Sham control rats underwent all surgical procedures without FPI. Opioid analgesia (Ethiqa XR) was administered subcutaneously for 72 h of postoperative coverage.

2.3. EEG electrode implantation and acquisition

2.3.1. Tethered EEG (TC-001)

Epidural electrodes were implanted 14–15 days after injury. Briefly, 1-mm-diameter stainless steel screw electrodes were implanted through 0.75-mm-diameter guiding craniotomies. The full electrocorticography (ECoG) montage consisted of five epidural electrodes (see Fig. 2A): a reference electrode placed midline in the frontal bone and two electrodes per parietal bone placed at coordinates bregma 0 mm and ± 6.5 mm, 4.5–5 mm from the midline. Three anchoring screws (one frontal and two occipital) were implanted to help secure the headset. All electrodes were connected through an insulated wire to gold-plated pins in a plastic pedestal (PlasticsOne Inc., Roanoke, VA). Parts of the craniotomy not covered with thick connective tissue were covered with biocompatible silicone (Kwik-Cast., WPI, Sarasota, FL). The entire assembly was then cemented onto the skull with a measured amount of dental acrylic (Jet, Lang Dental Manufacturing Co., Wheeling, IL) and further secured with VetBond (World Precision Instruments, Sarasota, FL) adhesive.

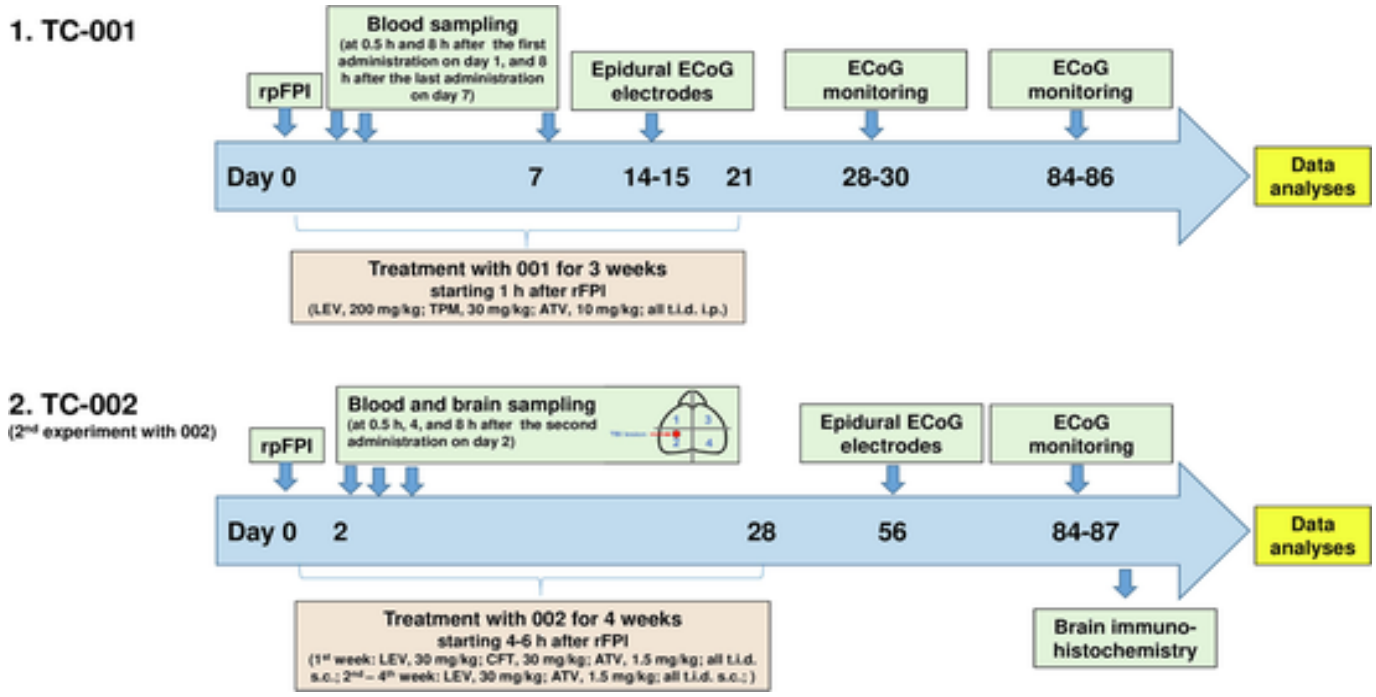

Fig. 1. Schematic illustration of the experiments with TC-001 (LEV, TPM, ATV) and TC-002 (LEV, ATV, CTX; main experiment) in rats. Blood and brain sampling was performed in separate groups of rats. See text for details.

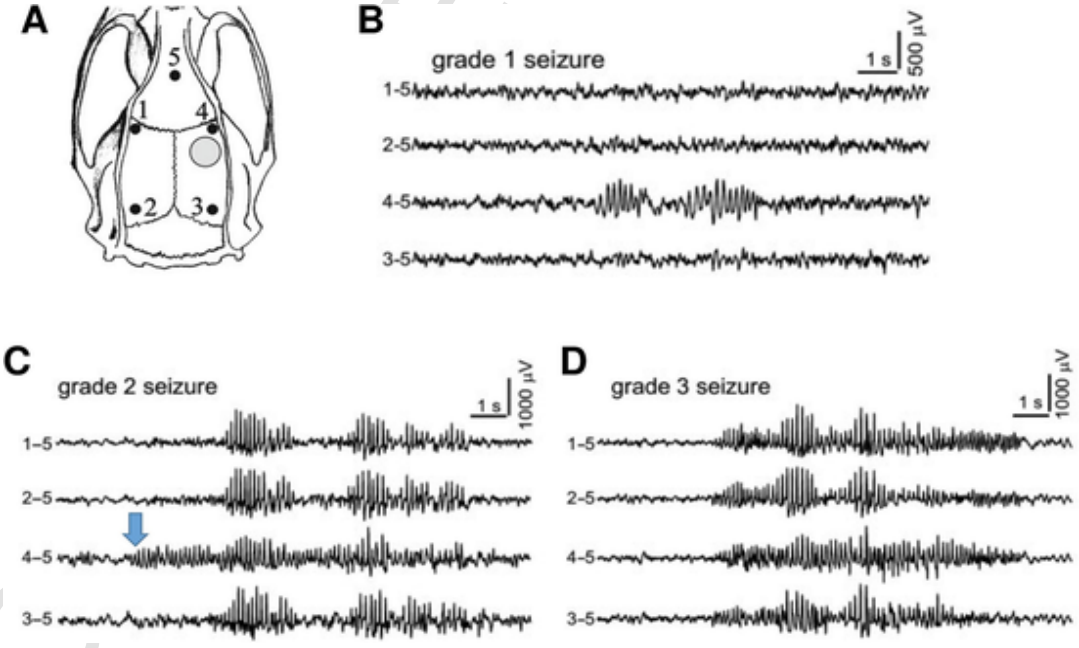

Fig. 2. Representative late spontaneous electrocorticographic seizures recorded in the FPI model. A: The montage used to record the multichannel electroencephalogram. Numbered black dots indicate electrode locations. The perilesional electrode (4) is located just rostral to the FPI craniotomy, which is indicated by a circle. B: A focal non-spreading (grade 1) seizure that is detected exclusively by the perilesional electrode. C: A spreading (grade 2) seizure that is first detected by the perilesional electrode (arrow) and then spreads to the contralateral cortex. (D) A spreading (grade 3) seizure with seizure onset detected simultaneously on multiple channels. The figure was modified from D'Ambrosio et al. (2009).

2.3.2. Wireless EEG (TC-002)

Rats were implanted with wireless telemetry transmitters (PhysioTel ETA-F10; Data Sciences International, St. Paul, MN) four (higher dose of TC-002) or eight weeks (reduced dose of TC-002) after FPI, with the active electrode over perilesional cortex 2 mm posterior to the FPI craniotomy, and reference electrode over the contralesional olfactory bulb (Hameed et al., 2023), to record one-channel continuous video-EEG (sampling rate: 1000 Hz), core-body temperature (0.1 Hz), and

home-cage locomotion activity (0.1 Hz) (Dhamne et al., 2017; Kelly et al., 2018).

2.4. Treatment groups

Immediately after FPI, injured animals were randomly assigned to either a vehicle or a drug cocktail. Treatment started 1 h (TC-001; first experiment with TC-002) or 4–6 h (second experiment with TC-002) after injury and continued for 21 (TC-001) or 28 (TC-002) days according to the dosing protocol verified in the tolerability studies (see below). Additional animals were included to account for intrinsic post-traumatic mortality, technical failure for epidural electrode implantation, and electrode loss over 3 months; so the final group size upon commencement of ECoG or EEG monitoring was 17 vehicle controls and 14 drug-treated rats for TC-001, 6 injured controls and 6 drug-treated injured rats for the first ("high-dose") TC-002 experiment, and 5 sham injured, 7 injured controls and 7 drug-treated injured rats for the second (reduced-dose) TC-002 (see also Table S1).

2.4.1. Treatment with TC-001

Prior to the efficacy study with TC-001 (a combination of LEV, TPM, and ATV), we examined whether the triple combination is tolerated by rats when administered after FPI. Based on previous epilepsy prevention studies in the IHK mouse model of mTLE (Welzel et al., 2021), the drugs were administered t.i.d. at the following i.p. doses: LEV, 200 mg/kg; TPM, 30 mg/kg; ATV (used as sodium salt), 10 mg/kg, respectively. All drugs were prepared fresh in 0.3 % meglumine in sterile water for injection (SWFI) as reported recently (Rundfeldt et al., 2023). A group of 14 FPI rats was treated with this cocktail for one week. Treatment was started at 1 h after FPI. Mortality, body weight, and general behavior (such as locomotor activity, posture, and grooming) of the rats were examined during treatment. A group of 15 vehicle (0.3 % meglumine)-treated FPI rats was used as a control. As reported recently (Rundfeldt et al., 2023), all treated animals had normal grooming behavior, activity level, and body weight growth, indicating an absence of distress. Furthermore, mortality was the same as in vehicle controls. Thus, we chose this drug combination at the described doses and dose intervals for the efficacy study.

2.4.2. Treatment with TC-002

The tolerability of TC-002 was tested in healthy rats before the experiments in injured rats. No safety issues were observed. In a first ("high-dose") pilot experiment with TC-002, we administered the combination of ATV (3 mg/kg t.i.d.), LEV (60 mg/kg t.i.d.), and CTX (60 mg/kg t.i.d.) in 0.3 % meglumine in sterile water at the same doses as in the previous mouse study in the IHK model (Welzel et al., 2021), but prolonged the duration of treatment from 5 days (mouse study) to 4 weeks to account for the longer latent period in the FPI rat model (Eastman et al., 2021; Hameed et al., 2023). To avoid local irritation in the abdominal cavity by too many i.p. administrations, drugs were injected subcutaneously (s.c.). Treatment started 1 h after FPI. As described in the Results, the treatment did not exert any antiepileptogenic effects compared to vehicle controls, but rather a pro-epileptogenic effect as previously observed with a higher dose of the triple combination in mice (Welzel et al., 2021).

We, therefore, decided to (i) reduce the doses by 50 % (based on a mouse:rat scaling factor of 2 as proposed by Nair and Jacob, 2016), (ii) start treatment ~4 h after FPI (based on the BRV study by Eastman et al., 2021 in the rat FPI model), and (iii) include CTX only in the first week of treatment to avoid potential toxicity because of prolonged CTX administration. For this experiment, rats were randomly divided into three experimental groups as follows: (1) Sham TBI; (2) FPI-vehicle: s.c. 0.3 % meglumine in SWFI t.i.d.; and (3) FPI-TC-002: ATV: 1.5 mg/kg s.c. t.i.d.; LEV: 30 mg/kg s.c. t.i.d.; CTX: 30 mg/kg s.c. t.i.d. for the first week, and ATV and LEV only for an additional 3 weeks.

Injured animals receiving TC-002 in both the high-dose and reduced-dose arms exhibited normal grooming behavior, activity level, and body weight growth as they recovered from FPI compared to vehicle controls. Furthermore, mortality in the reduced-dose TC-002 arm was the same as in vehicle controls (Table S1).

2.5. EEG monitoring and seizure identification

2.5.1. Tethered ECoG (TC-001)

ECoG was acquired continuously in 48-h epochs at 4 and/or 12 weeks after FPI. We have previously shown that there is little advantage to monitoring longer than 48 h because the FPI rat model used here does not exhibit the seizure clustering that is observed in chemical (e.g. kainate, pilocarpine) models of acquired epilepsy (Eastman et al., 2015).

Animals were tethered to the amplifier headstage. Brain electrical activity was amplified (×5000) and filtered (0.3 Hz high-pass, 300 Hz low-pass) using a Neurodata 12 or an M15 amplifier (Grass Instruments, Quincy, MA) acquired at 600 Hz per channel on computers equipped with SciWorks 4.1 or Experimenter V3 software (Datawave Technologies Inc., Longmont, CO) and DT3010 acquisition boards (DataTranslation Inc., Marlboro, MA). Videos were recorded in either VHS or in digital format using digital cameras. Each camera monitored a maximum of two cages (one animal per cage). The seizures in this model have been extensively characterized (see D'Ambrosio et al., 2004; Curia et al., 2011; and, especially, D'Ambrosio et al., 2005, 2009).

Primary analyses of ECoG data were conducted blind to subject, treatment, and any other treatment parameters. ECoG was visualized in Matlab (MathWorks Inc., Natick, MA) and manually scrolled offline. This approach is laborious and requires expert raters, but it permits reliable analysis of all seizure activity - and its spread - generated by the epileptic focus, and it is the approach used to evaluate human ECoG data. Seizure onset was characterized by 1) focal trains of spikes, with each spike lasting about 150 ms, clearly distinct from baseline; 2) a sudden increase in spectral power in the h band over the baseline (D'Ambrosio et al., 2004; Ikeda et al., 2009; Butler et al., 2013); and 3) simultaneous stereotyped ictal behavioral changes according to a behavioral scale previously described (D'Ambrosio et al., 2009; see also section 3.1) and according to the clinical practice of seeking evidence of abnormal neuronal activity paired to behavioral signs (Fisher et al., 2005; D'Ambrosio et al., 2009; D'Ambrosio and Miller, 2010a, 2010b). Identified seizures lasted from 1 s to over 10 s. Events occurring within 3 s of each other were defined as a single seizure. For the present study, only the paroxysmal ECoG events were used for the analysis of spontaneous seizures because, as described in section 3.1, most of the behavioral changes occurring during the paroxysmal ECoG events were so subtle that they could not be reliably assessed in the videos but best by direct observation of the animals. As a consequence, a reliable post hoc analysis of behavioral alterations in the videos of the video-EEG monitoring periods is difficult and associated with errors.

The following data were extracted for each seizure: 1) onset time, 2) duration, and 3) ECoG channel(s) at which the event started and spread to. The effects of drug treatment were assessed based on a comparison of seizure frequency (events/h), seizure incidence (proportion of rats that exhibited seizures), time spent seizing (seconds/h), and proportion of spreading seizures between treated groups and untreated controls. Three types of ECoG seizures were recorded (D'Ambrosio et al., 2009): Grade 1 seizures originating from the peri-lesion neocortical area and being limited to it (i.e., non-spreading seizures; Fig. 2B); grade 2 seizures originating from the peri-lesion neocortical area and then spreading to other sites (Fig. 2C); and grade 3 seizures appearing simultaneously at multiple sites (Fig. 2D). For the present analyses, grade 2 and 3 seizures were considered spreading seizures.

In addition to analyzing the incidence and frequency of all seizures independent of their duration (see Results), we separately analyzed the data for seizures with a duration ≥5 s to consistently use a single duration criterion that allows a cross-comparison of data obtained for TC-001 and TC-002 (see section 2.5.2).

2.5.2. Wireless EEG (TC-002)

One-channel wireless EEG, sampled at 1000 Hz and synced with video, was recorded differentially between the reference and active electrodes either weekly from 5 to 12 weeks (higher dose of TC-002) or once at 12 weeks (reduced dose of TC-002) after FPI. All data were acquired over a period of 48 h per time point using the PhysioTel implantable telemetry platform and Dataquest ART acquisition software (Data Sciences International, MN). All video EEG recordings were scored offline for seizures using an automated seizure detection algorithm (Neuroscore software; DSI) wherein individual spike characteristics such as amplitude, duration, frequency, and inter-spike intervals were used to differentiate seizures from interictal spikes or electrical and mechanical artifacts (Dhamne et al., 2023). Based on the results of the experiments with TC-001, which indicated that duration-based seizure definition (ranging from ≥1 to ≥10 s) did not significantly affect the outcome of treatment (see section 3.1), we decided to only analyze electrographic seizures of ≥5 s for the experiments with TC-002. This value is consistent with prior rodent experiments (Dhamne et al., 2023; D'Ambrosio et al., 2009) and human studies aimed to define a minimal spike train duration that can reliably be considered a seizure (Antwi et al., 2019). Only for the experiment with the higher dose of TC-002, we also analyzed seizures of ≥10 s duration because we observed that the incidence of these seizures was increased by the treatment (see Results).

Pursuant to the automated spike counts, all traces and detected events were also reviewed by blinded visual inspection of the marked EEG segments. Marked seizures were then verified against the real-time videos and spectral EEG metrics. As described in section 2.5.1., clinical corelates (e.g., freezing and facial automatisms) associated with EEG seizures could not be reliably assessed in our experimental protocol since (1) the animal snout was often out of camera view, and (2) the clinical appearance of the events was subtle and would require direct observation. We note that in instances when the animal was in adequate camera view, behavioral arrest was evident – however, since this was a minority of paroxysmal events, analyses reported here are based on electrographic seizures.

Importantly, we have previously reported that seizures as described here are not present in sham-injured age-matched male Sprague-Dawley rats (D'Ambrosio et al., 2009).

2.6. Measurement of drug plasma concentrations

In additional groups of rats, which were treated for one week with TC-001 or TC-002, plasma drug levels were determined in blood samples drawn from the tail vein. In the TC-001 study, blood was withdrawn at 0.5 h and 8 h following the first administration on day 1 and 8 h after the last administration on day 7. In the first TC-002 study, blood was withdrawn at 0.5 h and 8 h following the first administration on day 1, as well as in the morning before the first dosing on days 2, 5, and 7, and 0.5 and 8 h after the last administration on day 7. In the second TC-002 study, blood samples and brain tissue were collected from 3 rats each at 1, 4, and 8 h following the first administration on day 2.

Blood (200–500 ml) was collected in lithium-heparin or potassium ethylenediaminetetraacetic acid (EDTA)-coated tubes and stored on crushed ice before centrifugation (10 min at 1500 ×*g*) in a chilled rotor within 1 h of collection. Plasma samples (100–250 ml) were transferred to 0.5 ml microcentrifuge tubes and stored at −80 °C prior to analysis.

TC-002 brains were dissected into 4 quadrants (as illustrated in Fig. 1). One quadrant (#2) contained the lesioned cortex (because FPI may impair the ipsilateral blood-brain barrier [BBB]), while quadrant #1 contained the ipsilesional forebrain and quadrants #3 and #4 the contralateral parts of the brain, respectively. Quadrants were transferred to individual 2 ml tubes (Eppendorf, CT) and flash-frozen in liquid nitrogen before being stored at −80 °C. Plasma and brain drug levels were determined by ultra-performance liquid chromatography-mass spectrometry (LC-MS) (TC-001: Chemical Analytical Facility Core, Environmental and Occupational Health Sciences Institute, Rutgers University, NJ; TC-002: Department of Experimental and Clinical Pharmacology, College of Pharmacy, University of Minnesota, MN).

2.7. Histology (reduced-dose TC-002 experiment)

2.7.1. Perfusion of cortical tissues

Deeply anesthetized rats were transcardially perfused with PBS followed by 4 % paraformaldehyde (PFA), as previously described (Hameed et al., 2023). Harvested brains were then immersion-fixed in 4 % PFA at 4 °C for 24 h before being cryopreserved in 30 % sucrose. Cryoprotected brains were rapidly frozen in Tissue-Plus OCT Compound (Thermo Fisher Scientific, Waltham MA) and stored at −80 °C for at least 48 h before sectioning.

2.7.2. Immunohistochemistry

Free-floating coronal sections (30 μm) were blocked in 10 % goat serum and 0.1 % Triton X-100 in PBS for one hour, and then incubated overnight at 4 °C with primary antibodies (parvalbumin-positive interneuron [PVI]: anti-parvalbumin antibody; Swant, Marly, Switzerland; perineuronal net [PNN]: biotinylated *wisteria floribunda* agglutinin [WFA]; MilliporeSigma, St Louis MO) followed by Alexa Fluor conjugated secondary antibodies for one hour at room temperature (PVI: anti-guinea pig Alexa Fluor 488; PNN: streptavidin Alexa Fluor 594; Thermo Fisher Scientific, Waltham MA) (MacMullin et al., 2020; Hameed et al., 2023). Stained sections were mounted using Fluoromount medium containing 4′,6′-diamidino-2-phenylindole (DAPI) nuclear counterstain (Southern Biotechnology, Birmingham AL). All processing and staining steps were performed under identical conditions using the same batch of buffers to minimize inter-sample variability.

2.7.3. Image acquisition

Perilesional sites (1 mm lateral from the interhemispheric fissure) were identified. Confocal images were acquired at 10× magnification using FV10-ASW software (v2.1C) on an FV1000 confocal laser scanning microscope (Olympus Corporation, Tokyo, Japan) with the following parameters: Channel one: 488 nm laser power = 2 %, Dye = Alexa Fluor 488, PMT voltage = 465, PMT gain = 1; Channel two: 561 nm laser power = 5 %, Dye = Alexa Fluor 594, PMT voltage = 585, PMT gain = 1. Individual channels were acquired sequentially, and at least four sections were imaged per rat.

2.7.4. Cell count

Images were analyzed using ImageJ software as described previously (Hsieh et al., 2017; MacMullin et al., 2020; Hameed et al., 2023). First, a 400 μm wide region of interest corresponding to layers I-VI was selected in the middle of the imaging field. Identical threshold settings and filters for size (50–5000 μm^2) and circularity (0–1.0) were then applied to all images. Structures positively stained for PV and/or WFA (PNN) were identified and visually confirmed to be cells using DAPI nuclear counterstaining, and automated counts were then recorded.

2.7.5. PV intensity

To quantify PV content in individually identified PV+ cells, images were overlaid with a PV immunofluorescence channel using ImageJ, and intensity per cell was measured. PV intensity data were normalized to sham controls for analysis.

2.8. Network analysis of brain protein targets of TC-002

To explore known and predicted interactions between brain protein targets of LEV, ATV, and CTX, the STITCH database (http://stitch.embl.de/; version 5.0) for interaction networks of chemicals and proteins was used (Szklarczyk et al., 2016). STITCH ('Search Tool for Interacting Chemicals'), in its fifth release, encompasses ~10 million proteins from 2031 eukaryotic and prokaryotic genomes. Its chemical space includes 430,000 compounds (not including different stereoisomers) and 1.6 billion interactions (Szklarczyk et al., 2016). For the present analysis, the species was limited to the brain of humans, because the system does not allow tissue-specific analyses for rats. However, running the same drug combination for rats yielded the same protein targets plus additional targets in peripheral tissues (not illustrated).

2.9. Statistics

Group sizes for the experiment with TC-001 gave 80 % power to detect either a 60 % decrease in seizure incidence or a 90 % decrease in seizure frequency, with $p < 0.05$ (Eastman et al., 2011, 2015). Group sizes for the pilot experiments with TC-002 gave 80 % power to detect the prevention of spontaneous seizures, with $p < 0.05$. For statistical analyses of incidence data, Barnard's test was used. PVI counts were compared between groups using the Brown-Forsythe & Welch ANOVA with Dunnett T3.0 post-hoc tests. Seizure frequencies were analyzed by the Mann-Whitney *U* test, and per-cell PV intensity was compared using an unpaired *t*-test. Differences in plasma drug levels at different times after administration in the same group of rats were analyzed by the Wilcoxon signed rank test. A $P < 0.05$ was considered significant.

3. Results

3.1. A combination of LEV, TPM, and ATV (TC-001) does not prevent or modify the development of posttraumatic epilepsy in a rat model

As reported previously (D'Ambrosio et al., 2009), the FPI protocol used for the experiment resulted in the development of spontaneous recurrent ECoG seizures within 4 weeks in about 70 % of vehicle-treated controls (Fig. 3A). Most of these seizures were non-spreading (grade 1) seizures that were detected exclusively by the perilesional electrode (Fig. 2B). A proportion (median 0.14; Fig. 3E) of the seizures were spreading (grade 2 and 3) seizures that spread to the contralateral cor-

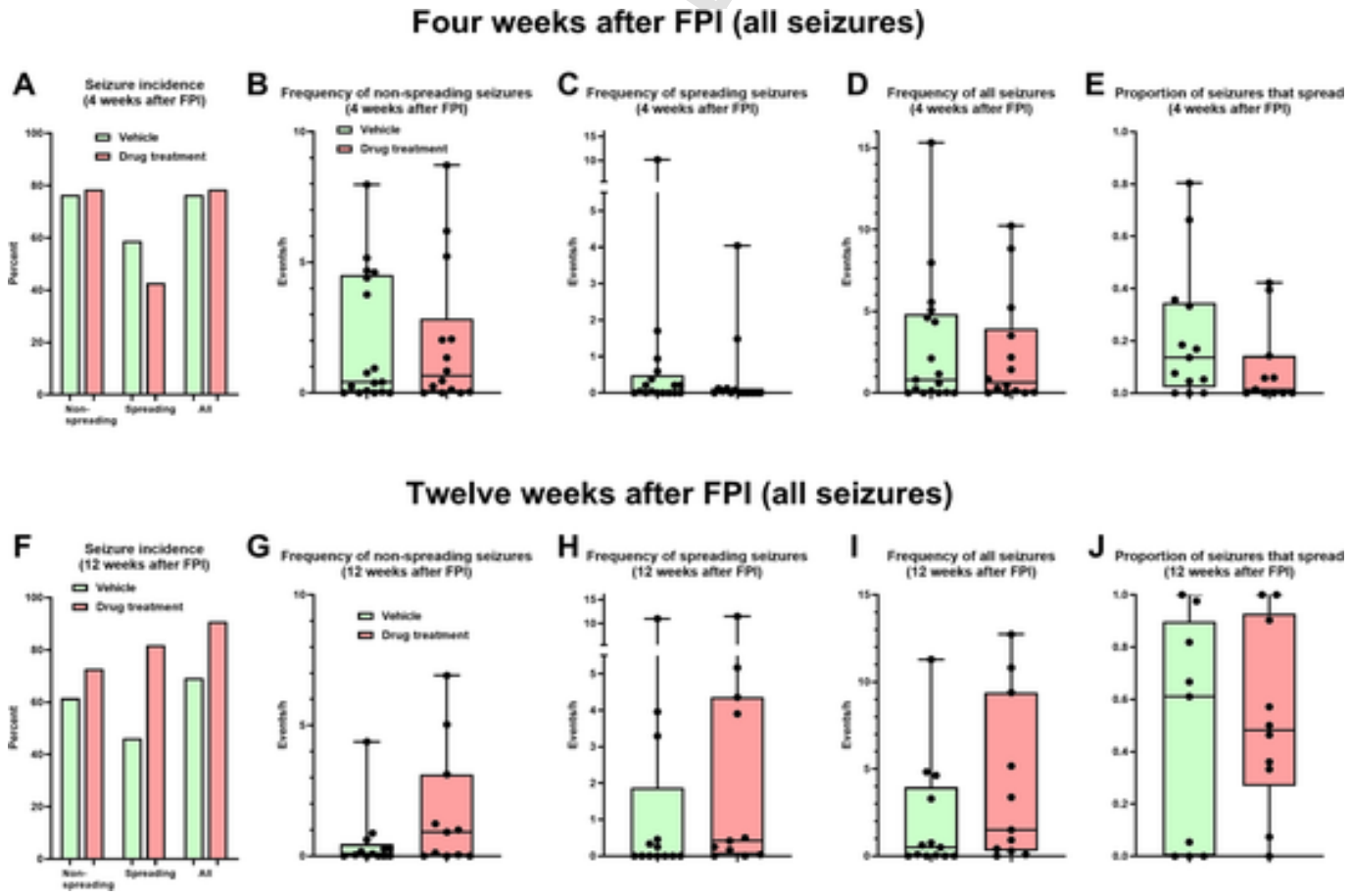

Fig. 3. The effect of TC-001 (LEV, TPM, ATV) on the incidence and frequency of spontaneous recurrent electrocorticographic (ECoG) seizures recorded 4 and 12 weeks after FPI in rats. Data are from 17 vehicle-treated and 14 drug-treated rats. Some rats lost their electrode head assemblies before the 12-week monitoring period, which reduced the sample size to 13 (vehicle) and 11 (drug), respectively. Except for the seizure incidences in A and F, all data are shown as boxplots with whiskers from minimal to maximal values; the horizontal line in the boxes represents the median value; in addition, individual data are shown. All seizures independent of their duration (see Methods) were used for the analyses. Seizures were differentiated into non-spreading and spreading (see Fig. 2). Statistical analyses did not indicate any significant effect of the drug treatment. A-E illustrate data determined at 4 weeks, and F-J at 12 weeks after FPI. A and F: Incidence of non-spreading, spreading, and all spontaneous recurrent ECoG seizures. B and G: Frequency of non-spreading seizures. C and H: Frequency of spreading seizures. D and I: Frequency of all seizures. E and J: Proportion of seizures that spread. Note the significant increase in the proportion of seizures that spread at 12 weeks (J) vs. 4 weeks (E) after FPI in vehicle controls ($P = 0.0469$) and drug-treated rats ($P = 0.0039$).

tex (Fig. 2C,D). At 12 weeks after FPI, the proportion of spreading seizures had increased to 0.61 (P = 0.0469; Fig. 3J), demonstrating that PTE in this model is progressive as previously reported (D'Ambrosio et al., 2005; Curia et al., 2011).

Daily treatment with a combination of LEV, TPM, and ATV (TC-001) over 3 weeks, starting 1 h after FPI, did not significantly alter the incidence or frequency of spontaneous recurrent ECoG seizures (Fig. 3). There was a trend for reduced incidence and proportion of spreading seizures in TC-001-treated rats at 4 weeks after FPI (Fig. 3A,E), but this was not observed at 12 weeks (Fig. 3F,J). The median proportion of seizures that spread in the drug-treated rats was 0.014 at 4 weeks but 0.48 at 12 weeks (P = 0.0039), demonstrating the progression of the epilepsy despite treatment. Also, time spent in seizures was not significantly altered by treatment (not illustrated).

For the data in Fig. 3, analyses were performed for all seizures independent of their duration. In Fig. 4, seizure incidence was analyzed as a function of duration-based seizure definition (i.e., the minimum seizure duration), both for all seizures (spreading, non-spreading) and for spreading seizures. As shown in Fig. 4, the apparent incidence of seizures tended to decrease with the stringency of seizure definition. Drug treatment tended to decrease the incidence of spreading seizures at 4 weeks, but an opposite trend was observed after 12 weeks. None of these trends was statistically significant.

In addition to analyzing the incidence and frequency of all seizures independent of their duration (Fig. 3), we separately analyzed only seizures of ≥5 s duration to allow for easy cross-comparisons of data obtained with TC-002 (see section 3.2). As shown in Fig. 5A,F, the incidence of ECoG seizures ≥5 s in duration in vehicle controls was 65 % at 4 weeks and - due to the loss of some rats - 54 % at 12 weeks after FPI. The median proportion of spreading seizures increased from 0.43 at 4 weeks (Fig. 5E) to 0.94 at 12 weeks (Fig. 5J), substantiating the progressive nature of PTE in this model. Treatment with TC-001 did not significantly alter the incidence, frequency, or progression of spontaneous recurrent ECoG seizures (Fig. 5).

We also examined whether the dosing regimen chosen for treatment with TC-001 resulted in therapeutically relevant plasma levels. LEV, TPM and ATV are rapidly eliminated by rats with half-lives of about 2 h (Löscher and Klein, 2021; Rundfeldt et al., 2023), so the triple drug combination was administered three times daily at 8 h intervals at 200 mg/kg (LEV), 30 mg/kg (TPM), and 10 mg/kg (ATV), respectively, As shown in Fig. 6A, this dosing regimen resulted in LEV plasma levels above (peak levels) or within (trough levels) the plasma concentration range (12–46 μg/ml) known from patients with epilepsy (Patsalos et al., 2008) and severe TBI treated with LEV 55 mg/kg/day for prevention of PTE (Klein et al., 2012). Following 7 days of t.i.d. administration, trough levels of LEV were similar to those determined 8 h after the

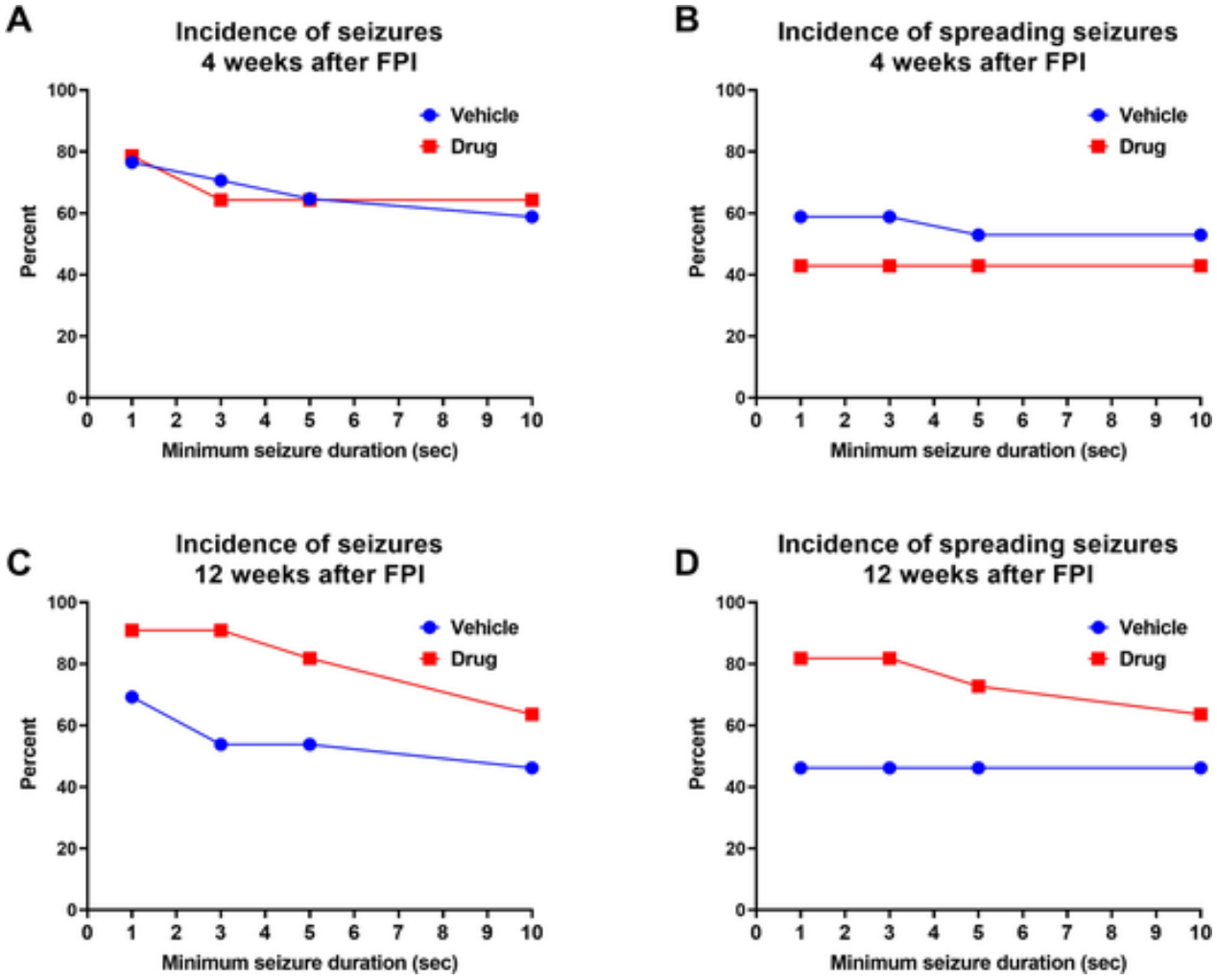

Fig. 4. Incidence of spontaneous recurrent electrocorticographic seizures as a function of duration-based seizure definition. As described in Methods, based on duration, the incidence of seizures with ≥1 s, ≥3 s, ≥5 s, and ≥ 10 s duration is shown. The apparent incidence decreases with the stringency of the seizure definition. Treatment with TC-001 (LEV, TPM, ATV) after FPI does not significantly alter seizure incidence.

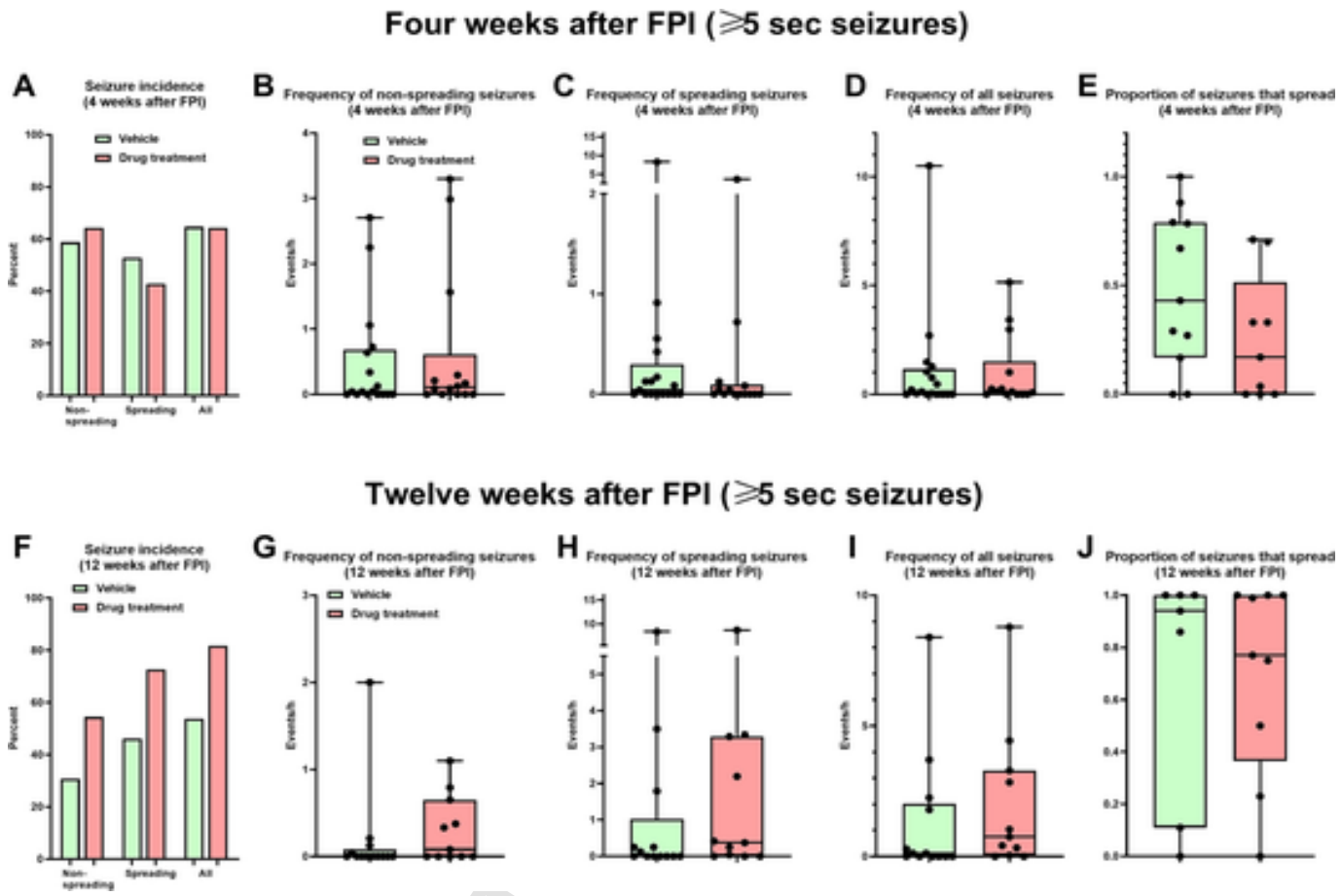

Fig. 5. The effect of TC-001 (LEV, TPM, ATV) on the incidence and frequency of spontaneous recurrent electrocorticographic (ECoG) seizures recorded 4 and 12 weeks after FPI in rats. In contrast to Fig. 3, only seizures of ≥5 s duration were used for the analysis to allow cross-comparison of data obtained for TC-001 and TC-002 (see text). Statistical analyses did not indicate any significant effect of the drug treatment. See Fig. 3 legend for further details.

first administration (Fig, 4 A), thus excluding drug accumulation or metabolic tolerance. Concerning TPM plasma levels, trough levels determined at 8 h following drug administration were below the therapeutic plasma concentration range (5–20 μg/ml) both on day 1 and day 7 of the treatment period (Fig. 6B). Peak levels were above this range, and Fig. 6B indicates that therapeutic plasma levels were maintained for at least 4–6 h per day. Trough levels of TPM determined on day 7 were not significantly different from those of day 1. Concerning plasma levels of ATV, the dotted area in Fig. 6C indicates the range of drug plasma levels (5.4–23.7 ng/ml) in ATV-treated patients with hyperlipidemia (Farahani et al., 2009). Plasma levels of half of the rats were above or within this range throughout the day, whereas the other half was slightly below this range. Trough levels of ATV determined on day 7 were not significantly different from those of day 1.

For comparison with drug plasma levels in rats, Fig. 6D and E illustrate plasma levels of LEV and TPM in mice, determined in a previous study in mice in which the combination of these two drugs exerted antiepileptogenic effects in the IHK mouse model (Schidlitzki et al., 2020). The antiepileptogenic effect in the mouse model was obtained despite trough levels of both LEV and TPM being below the therapeutic plasma concentration range of patients with epilepsy. This indicates that maintenance of therapeutic plasma concentrations determined in patients with epilepsy is not needed to obtain an antiepileptogenic effect when drugs are administered in combination. Indeed, in contrast to the significant antiepileptogenic effect of the drug combination in the mouse model, LEV administered alone did not exert such an effect and the effect of TPM alone was lower than the effect of the combination, indicating a synergistic effect of the combination (Welzel et al., 2021). Thus, the lack of antiepileptogenic efficacy of the triple combination (TC-001) in the rat model was most likely not a consequence of too low trough levels of TPM (Fig. 6B). In this respect, we note that while doses to obtain an antiseizure effect in rodents are much higher than in humans (due to species differences in drug metabolism), plasma drug concentrations at effective doses are remarkably similar in rats, mice, and humans (Löscher, 2007; Löscher, 2016). However, we cannot exclude that the hypothesized pharmacodynamic synergy of the LEV + TPM drug combination in mice may not exist in rats, although a drug-drug protein interaction network analysis of TC-001 by STITCH did not indicate any obvious differences between mice and rats (not illustrated).

The comparison of drug plasma levels in mice and rats illustrated in Fig. 6 demonstrated that - although the same drug doses were administered in both species – peak and trough levels of LEV in rats were about twofold higher than those in mice. This can be explained by the species differences in metabolic rate and body surface area, based on which a factor of ~2 has been proposed for mouse:rat allometric scaling for dose conversion (Nair and Jacob, 2016). However, no such species differences in peak and trough plasma levels were observed for TPM (Fig. 6).

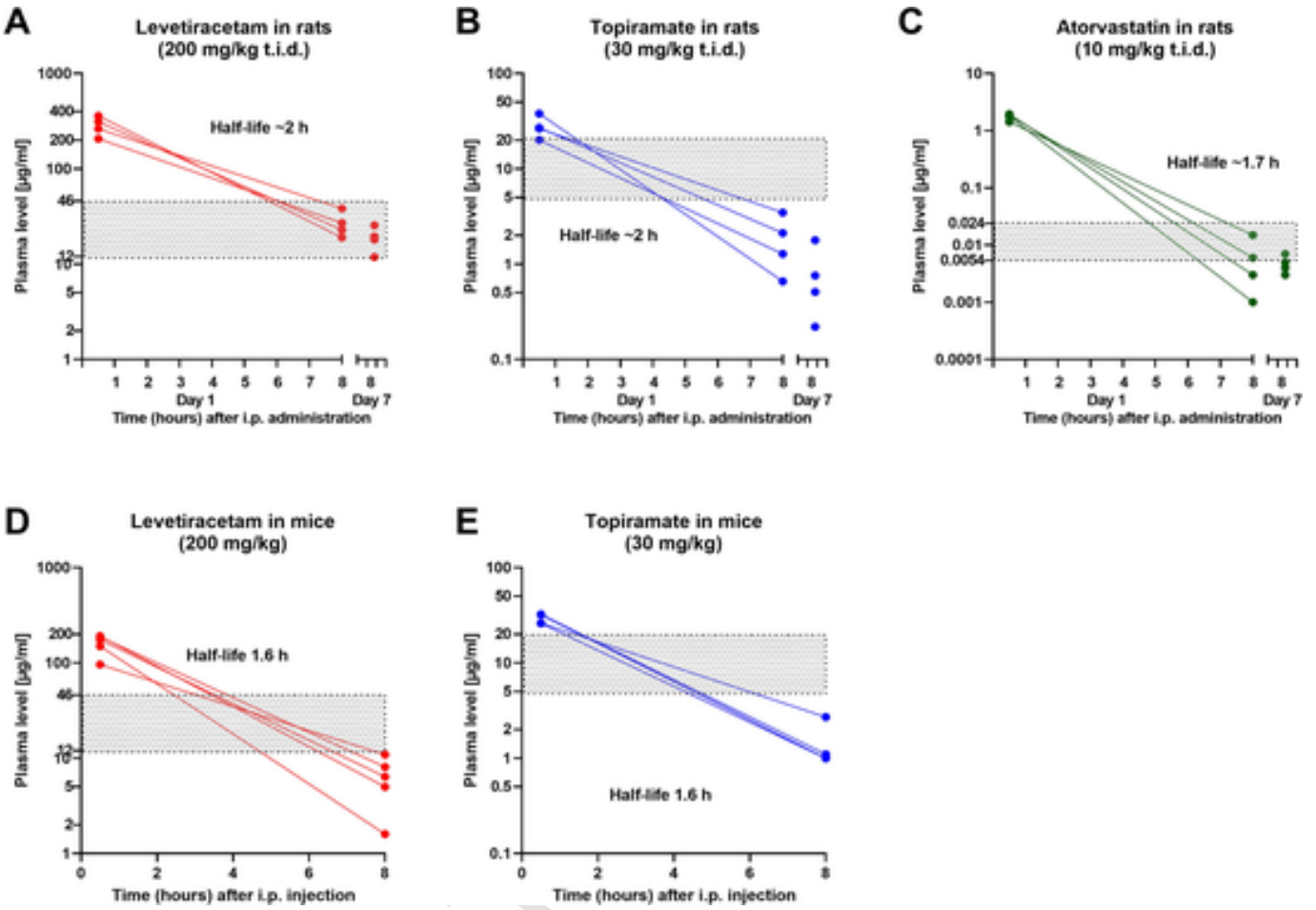

Fig. 6. Pharmacokinetics of LEV (A), TPM (B), and ATV (C) following i.p. administration of a triple-drug solution in meglumine in a group of four rats. The three drugs were dissolved in an aqueous solution of 0.3 % meglumine and administered at the following doses t.i.d.: TPM, 30 mg/kg; LEV, 200 mg/kg; ATV, 10 mg/kg, respectively. Blood was withdrawn at 0.5 h and 8 h following the first administration on day 1 and 8 h after the last administration on day 7. Individual data are shown. The dotted areas indicate the therapeutic plasma concentration range as determined in patients with epilepsy (LEV, TPM; Patsalos et al., 2008) or lipid-controlling patients (ATV; Farahani et al., 2009). Note the logarithmic scale of the y-axis. Plasma levels determined 8 h after the first and last drug administration were not significantly different. Average elimination half-lives indicated in the graphs were determined by PK Solutions (Summit Research Services, Montrose, CO). For comparison with rat data, plasma levels determined after a combination of LEV and TPM in mice are shown in D and E (Schidlitzki et al., 2020). Note the higher maximal and trough plasma levels of LEV in rats vs. mice despite the same dose is administered in both species.

3.2. A combination of LEV, ATV, and CTX (TC-002) dose-dependently affects the incidence of post-traumatic electrocorticographic seizures in the rat FPI model

In a first ("high-dose") pilot experiment with TC-002, in which the combination of LEV (60 mg/kg t.i.d.), ATV (3 mg/kg t.i.d.), and CTX (60 mg/kg t.i.d.) was administered at the same doses as in the previous mouse study in the IHK model (Welzel et al., 2021), the treatment did not exert any antiepileptogenic effects compared to vehicle controls but rather a pro-epileptogenic effect (Fig. 7) as previously observed with a higher dose of the triple combination in mice (Welzel et al., 2021). While there was no significant difference in the incidence of ECoG seizures ≥5 s at 3 months post-FPI (Fig. 7A), the incidence of seizures ≥10 s was significantly increased in drug-treated rats (Fig. 7B). In this experiment, we also examined the time course of occurrence of spontaneous seizures and observed a progressive increase in the frequency of ECoG seizures ≥10 s in drug-treated injured rats in the weeks following FPI (Fig. 7C). Drug-treated rats developed seizures (≥10 s) earlier and in larger proportions than vehicle-treated injured controls (Fig. 7D), indicating a pro-epileptogenic effect of TC-002. Moreover, early high-dose treatment was associated with a tendency for increased survival in the hours following injury (75 % vs. 60 %; Barnard's test, not significant [$P = 0.5978$]; Table S1), possibly resulting in an aggregation of more severely injured rats in the TC-002 group.

The drug plasma levels determined during treatment with TC-002 are shown in Fig. S1. Peak levels of LEV determined at 0.5 h after s.c. administration at day 1 and day 7 were above or within the range (12–46 µg/ml) following therapeutic doses of LEV in epilepsy patients, whereas most trough levels were below this range (Fig. S1A). Elimination half-life after s.c. injection was 3.68 ± 0.77 h (mean ± SEM of 5 rats), which is higher than the half-life determined after i.p. injection (see above). No significant accumulation of drug levels was observed during treatment. Peak ATV plasma levels were above the range of drug plasma levels (5.4–23.7 ng/ml) in lipid-controlling patients (Farahani et al., 2009), while trough levels were within this range (Fig. S1B). Elimination half-life of LEV after s.c. injection was 2.22 ± 0.37 h. No significant accumulation of drug levels was observed during treatment. Peak plasma levels of CTX were highly above the clinically therapeutic range (13–15 µg/ml; Pollock et al., 1982), whereas trough levels were mostly below this range (Fig. S1C). Elimination half-life after s.c. injection was 2.01 ± 0.6 h. No significant accumulation of drug levels was observed during treatment.

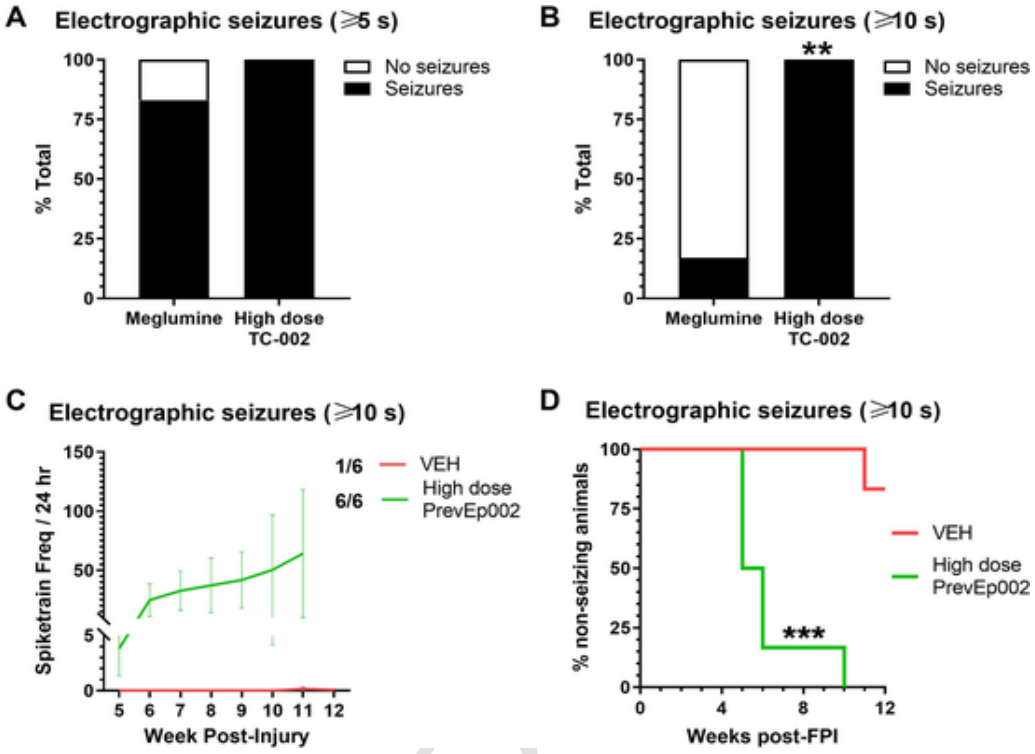

Fig. 7. The effect of high-dose TC-002 (LEV, ATV, CTX) on the incidence of spontaneous recurrent electrocorticographic (ECoG) seizures after FPI in rats. Data are from 6 vehicle-treated and 6 drug-treated rats. (A) Incidence of spontaneous recurrent EEG seizures ≥5 s. No significant group difference was observed. (B) Incidence of spontaneous recurrent EEG seizures ≥10 s. TC-002 significantly increased the cumulative incidence of spontaneous ECoG seizures 12 weeks after FPI (**$P = 0.002197$). (C) There was a progressive increase in the frequency of ECoG seizures ≥10s in drug-treated injured rats in the weeks following FPI. (D) Drug-treated rats developed seizures (≥10s) earlier and in larger proportions than vehicle treated injured controls (***$P < 0.001$).

As described in Methods, given the pro-epileptogenic effect observed in the pilot experiment with TC-002, we decided to (1) reduce the doses by 50 % (based on a mouse:rat scaling factor of 2 as proposed by Nair and Jacob, 2016), (2) start treatment ~4 h after FPI (based on the BRV study by Eastman et al., 2021 in the rat FPI model), and (3) include CTX only in the first week of treatment to avoid potential toxicity/pro-epileptogenic activity because of prolonged CTX administration. This treatment schedule significantly reduced the incidence of spontaneous recurrent ECoG seizures (Fig. 8A) greater than 5 s in duration, 12 weeks after injury (Fig. 8B).

When we combined the data of the two experiments with TC-002, the effect of treatment with the two dose schedules of TC-002 was significantly different (Fig. S2). However, as described in Methods, TC-002 dose was not the only difference between the two experiments - initial higher TC-002 dose studies were performed in older Wistar rats (P56–63), while the lower dose TC-002 studies were performed in younger Sprague Dawley rats (P32–36), so it is possible that the different efficacy results are due to age and/or strain differences. Furthermore, the lower dose treatment with TC-002 was administered starting 4–6 h after FPI, while in the first experiment, the higher dose was given starting 1 h after FPI. In addition, CTX treatment was included only in the 1st week as part of the second 'lower-dose' study vs. 4 weeks in the higher TC-002 dose study.

The drug plasma levels determined with the reduced doses of TC-002 are shown in Fig. 9. As expected, both peak and trough levels of LEV, ATV, and CTX were below those determined with the higher doses in the pilot experiment (Fig. S1). While LEV levels were within or slightly below the therapeutic range throughout the 8 h after s.c. administration (Fig. 9A), levels of ATV rapidly declined and were below the detection limit already at 4 h after administration (Fig. 9B). CTX plasma levels were above the therapeutic range at 1 and 4 h after administration, but below the detection limit at 8 h (Fig. 9C).

In this experiment, we also determined drug levels in the brain, both ipsilateral and contralateral to the site of injury (see Methods). As shown in Fig. 9D, brain levels of LEV at 1 and 4 h after injection were within the levels (7.0–21.2 μg/g) determined in brain samples resected from patients during epilepsy surgery (Rambeck et al., 2006), whereas brain levels at 8 h were below this range. The average brain:plasma ratio of LEV was 0.26 at 1 h, 0.52 at 4 h, and 0.49 at 8 h after administration.

For ATV, no reference brain levels were found in the literature. Brain levels in rats ranged between 5 and 13 ng/g at 1 and 4 h after administration but rapidly declined below the detection limit at 8 h (Fig. 9E). The average brain:plasma ratio of ATV was 0.41 at 1 h after administration.

Peak brain levels of CTX at 1 h were within the range (0.3–12 μg/g brain tissue) determined in patients who underwent surgery for cerebral tumors (Lucht et al., 1990). However, CTX brain levels rapidly declined thereafter and were below the detection limit at 4 h after administration (Fig. 9F). The average brain:plasma ratio of CTX was 0.0061 at 1 h after administration, indicating that less than 1 % of the CTX plasma level entered the brain.

Of note, presumed BBB disruption due to FPI did not appreciably alter drug penetration into the CNS, as all 4 brain quadrants exhibited similar levels of all three compounds (Fig. 9D-F).

3.3. A combination of ATV, LEV, and CTX (reduced-dose TC-002) exerts neuroprotective effects in the rat FPI model

On immunohistochemistry, there was a significant decrease in perilesional cortical PVI density 12 weeks after TBI compared to sham, and

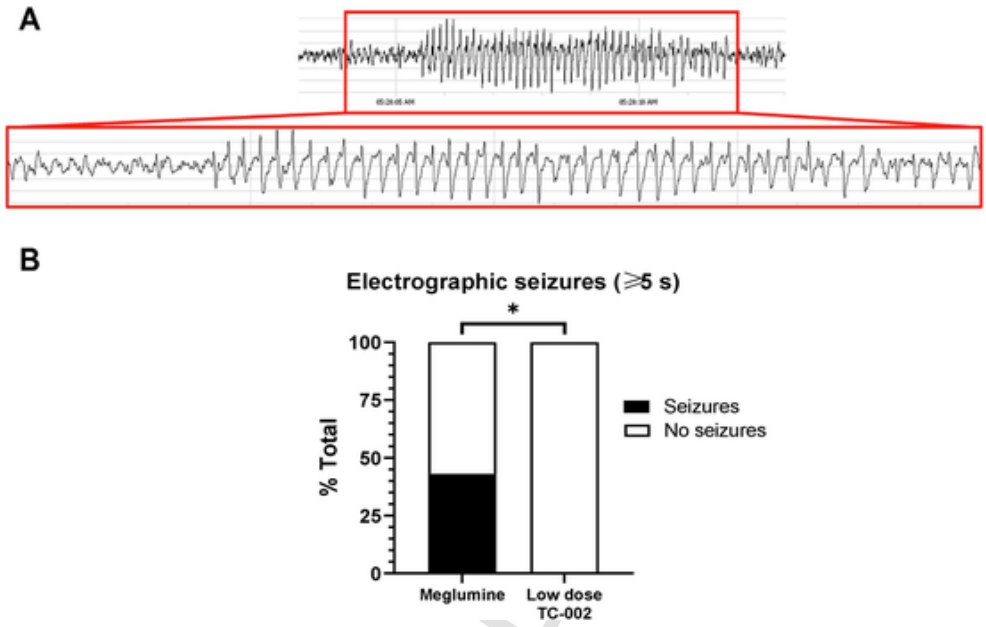

Fig. 8. The effect of a reduced dose of TC-002 (LEV, ATV, CTX) on the incidence of spontaneous recurrent electrocorticographic (ECoG) seizures ≥5 s recorded 12–16 weeks after FPI in rats. Data are from 7 vehicle-treated and 7 drug-treated rats. (A) Representative EEG seizure 12 weeks after FPI in a vehicle-treated, injured control animal. (B) Incidence of spontaneous recurrent EEG seizures: TC-002 treatment significantly decreased the incidence of spontaneous ECoG seizures (runs of spikes ≥5 s) 12–16 weeks after FPI. (*$p < 0.05$).

this loss was mitigated but not normalized with TC-002 treatment (Fig. 10). Frequency distribution of PV pixel intensity per PV-positive cell in perilesional cortex 12 weeks after TBI also showed a significant increase in mean per-PVI PV content in FPI-TC-002 rats compared to FPI-vehicle controls (Fig. 11). As shown previously for healthy cortex (Hsieh et al., 2017; Hameed et al., 2023), the majority of PVIs in sham controls were surrounded by a supportive PNN (labeled in green in Fig. 11B). Sham-treated FPI resulted in PNNs that appear "empty" i.e. without PVIs. Triple combination therapy partially reversed these findings.

3.4. Brain protein interaction network analysis of TC-002

To explore potential mechanisms related to the antiepileptogenic effect of TC-002, the known and predicted drug-drug brain protein interactions of LEV, ATV, and CTX were identified in silico, using the STITCH Database. As shown in Fig. S3, the drug-drug interaction analysis indicates a direct interaction between CTX and LEV as well as LEV and ATV but not CTX and ATV. More importantly, the three drugs interact in a large drug-brain protein network. Therefore a consequence of combined treatment with LEV, ATV, and CTX could be to impact a larger functional network of epilepsy-relevant brain proteins than each drug alone, providing a potential network pharmacology explanation for the observed antiepileptogenic and neuroprotective effects observed with this combination. Key targets identified by STITCH include the main brain targets of LEV (SV2 A [synaptic vesicle glycoprotein 2 A]), CTX (SLC1A2, the astrocytic glutamate transporter EAAT2), and ATV (HMGCR [3-hydroxy-3-methylglutaryl-CoA reductase], the rate-limiting enzyme in cholesterol biosynthesis). However, all three drugs and ATV in particular interact with various other brain proteins that are involved in epileptogenesis, including HMGB1 (*high mobility group box 1*), a key initiator of neuroinflammation following brain injuries leading to epilepsy (Ravizza et al., 2018); IL-1β (interleukin 1β), a prototypical inflammatory cytokine that is increased during epileptogenesis (Ravizza et al., 2024), the RAS homolog RHEB, which is enriched in brain and activates the protein kinase activity of mTORC1 (mechanistic target of rapamycin complex 1), a critical signaling pathway in epileptogenesis (Ravizza et al., 2024); furthermore, RAS proteins are involved in neuroinflammation (Fracassi et al., 2019); RAC1 and RAC3, small GTP binding proteins that are involved in the generation of oxidative stress (Fracassi et al., 2019); and the nuclear receptor PPARα (peroxisome proliferator-activated receptor alpha), which ATV activates to enhance the transcription of CREB (cAMP responsive element binding protein), driving the expression of neurotrophic factors such as brain derived neurotrophic factor (BDNF) and neurotrophin-3, both thought to be involved in the neuroprotetive effects of statins (Fracassi et al., 2019). Further potentially important brain protein targets of TC-001 are illustrated in Fig. S3 and explained in the figure legend.

4. Discussion

To our knowledge, this is the first POC study evaluating whether rationally chosen multi-targeted drug combinations can prevent epilepsy in an animal PTE model. While TC-001 (LEV, TPM, ATV) and a high dose of TC-002 (LEV, CTX, ATV) failed to prevent PTE in the rat FPI model, a pilot experiment with a reduced dose of TC-002 indicated that this drug combination is effective when using allometric scaling of doses to take into account the differences in mouse:rat body surface areas. At this reduced dose, TC-002 also partially prevented the loss of perilesional cortical PVI-positive neurons. This neuroprotective effect of TC-002 may contribute to the antiepileptogenic effect of TC-002.

We and others have previously shown that cortical PVIs, which represent close to 40 % of the cortical GABAergic inhibitory interneuron population (Rudy et al., 2011), are supremely vulnerable to post-traumatic metabolic changes (Moga et al., 2002; Cabungcal et al., 2013; MacMullin et al., 2020; Ruden et al., 2021; Hameed et al., 2023). PVIs have a high baseline firing rate and therefore produce high concentrations of reactive oxygen species (ROS) and thus oxidative stress, which is skewed toward toxic after TBI (Cantu et al., 2015; Yamamoto et al., 1999; Zhuang et al., 2019). Given their prominent role in maintaining cortical excitation:inhibition (E:I) balance (Cammarota et al., 2013; Sohal et al., 2009), the biased loss of this vulnerable cell population as

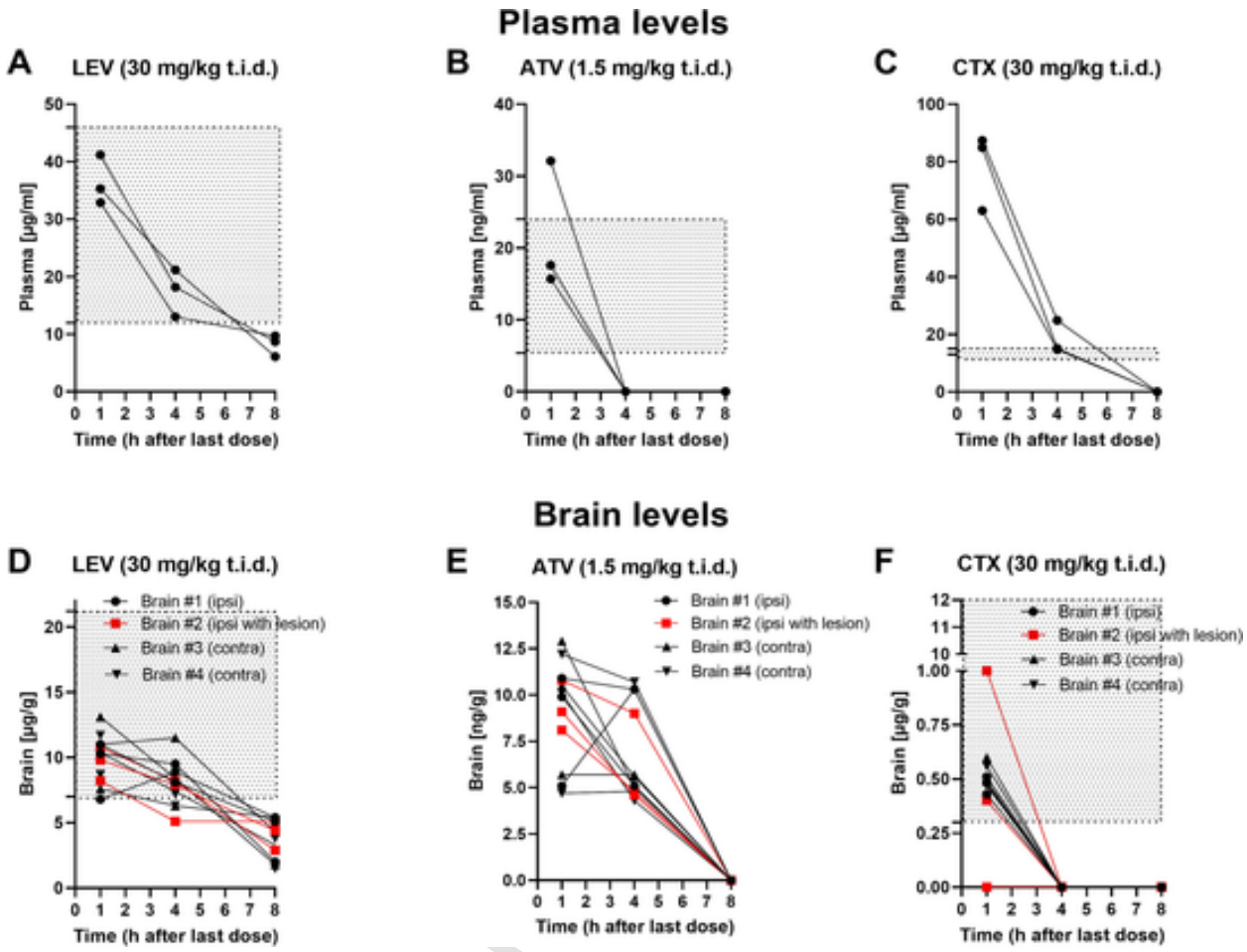

Fig. 9. Plasma and brain levels of LEV (A, D), ATV (B, E), and CTX (C, F) following s.c. administration of a triple-drug solution (TC-002; reduced doses) in meglumine in a group of three rats. The three drugs were dissolved in an aqueous solution of 0.3 % meglumine and administered at the following doses t.i.d.: LEV, 30 mg/kg; ATV, 1.5 mg/kg, and CTX, 30 mg/kg, respectively. Blood was withdrawn at 1 h, 4 h, and 8 h following the first administration on day 2. Individual data are shown. For plasma levels, the dotted areas indicate the therapeutic plasma concentration range as determined in patients with epilepsy (LEV; Patsalos et al., 2008), lipid-controlling patients (ATV; Farahani et al., 2009), or patients with infections (CTX; Pollock et al., 1982). As described in Methods, brain levels were determined in 2 ipsilateral and 2 contralateral quadrants; quadrant #2 contained the lesioned cortex. As shown in D—F, no obvious difference between brain levels determined in these quadrants was observed. The dotted area in D indicates the brain level range of LEV determined in patients during epilepsy surgery (Rambeck et al., 2006). The dotted area in F indicates the brain level range of CTX determined in patients undergoing tumor surgery (Lucht et al., 1990). For ATV, no reference brain levels were found in the literature.

seen after TBI (Hsieh et al., 2017; Hameed et al., 2019, 2023) may be a large contributor to PTE (Godoy et al., 2022).

In addition to neuroprotective activity, the drugs combined in TC-002 have several molecular MOAs that are relevant for antiepileptogenic efficacy (Table S2; Fig. S3). These include positive effects on GABAergic transmission (LEV), anti-glutamatergic effects (LEV, CTX), anti-inflammatory effects (LEV, ATV, CTX), and anti-oxidative stress effects (LEV, ATV, CTX) (Scicchitano et al., 2015; Rogawski et al., 2016; Yimer et al., 2019; Klein et al., 2020; Löscher, 2020; Löscher and Klein, 2022). Changes in these targets occur within hours to days after TBI, which is important for the timing of antiepileptogenic interventions (Löscher and Klein, 2022). An example is the astrocytic glutamate transporter 1 (GLT-1; the rodent analog of human EAAT2), the major mechanism for glutamate removal from synapses (Kim et al., 2011). FPI results in a decrease in GLT-1 expression, which, coupled with an increase in glutamate release from dead and dying neurons, causes an increase in extracellular glutamate (Goodrich et al., 2013). Neocortical GLT-1 gene and protein expression are significantly reduced for up to 6 weeks after FPI in rats, and this transient loss is mitigated by CTX (Goodrich et al., 2013; Hameed et al., 2019). If the FPI-induced decrease in GLT-1 is not prevented by CTX, the ensuing glutamate excitotoxicity and oxidative toxicity disproportionately damages vulnerable GABAergic PVI-positive inhibitory interneurons, resulting in a progressively worsening cortical E:I imbalance due to a loss of GABAergic inhibitory tone (Hameed et al., 2019). However, treatment with CTX alone did not prevent PTE in the FPI rat model but only reduced cumulative post-traumatic seizure duration (Goodrich et al., 2013). At high drug levels, CTX is also a weak $GABA_A$ receptor antagonist (Amakhin et al., 2018), which may explain why the higher dose of TC-002 exerted pro-epileptogenic effects in the present study. Similarly, a high dose of TC-002 was ineffective in the IHK mouse model of mTLE (Welzel et al., 2021).

Importantly, the antiepileptogenic and neuroprotective effect of the reduced dose of TC-002 in the rat FPI model of PTE observed here occurred at plasma and brain drug levels that were previously reported with therapeutic doses of LEV, and CTX in humans, which would facilitate dose finding for clinical studies. This was also the case for plasma levels of ATV; we are not aware of reports of human brain ATV levels. We also did not identify any previous report of rodent brain ATV levels following systemic administration, but such data exist for lovastatin,

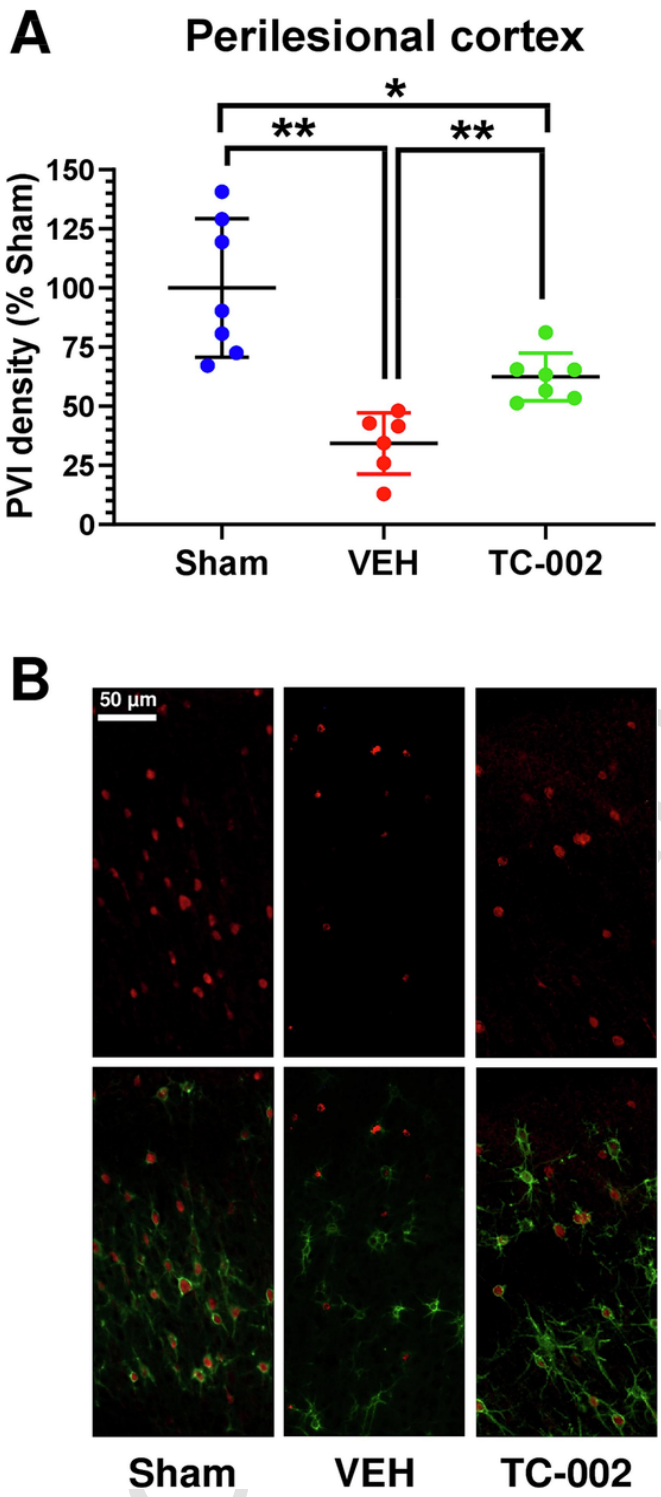

Fig. 10. The effect of TC-002 (LEV, ATV, CTX) on cortical parvalbumin-positive interneuron (PVI) density. (A) There was a significant decrease in perilesional cortical PVI density 12–16 weeks after FPI compared to sham, and this loss was mitigated but not normalized with ATV/LEV/CRO treatment. Individual data are shown with mean ± SD; *p < 0.05, **p < 0.01.
(B) Representative confocal images in perilesional cortex in all experimental groups (Sham, Vehicle, TC-002) 12–16 weeks after injury. Top row: PVI staining (red) is markedly decreased in both count and intensity following vehicle-treated FPI. Bottom row: in healthy cortex (sham), the majority of PVIs are surrounded by a supportive perineuronal net (PNN; green). Vehicle-treated FPI results in PNNs that appear "empty" i.e. without PVIs. Triple combination therapy partially reverses these findings. (For interpretation of the references to colour in this figure legend, the reader is referred to the web version of this article.)

Fig. 10.—*continued*

simvastatin, and pravastatin following oral administration in mice (Johnson-Anuna et al., 2005). Similarly, high brain perfusion was reported for the lipophilic statins simvastatin and lovastatin in rats, whereas the less lipophilic pravastatin did not cross the BBB in this species (Saheki et al., 1994). Regarding ATV, based on several physicochemical parameters related to BBB penetration, Sierra et al. (2011) concluded that this statin, which has a higher molecular weight (558) than simvastatin (436) and lovastatin (422), scarcely penetrates into the brain by passive diffusion. However, statins are substrates of organic anionic transporters (OATs), organic anion-transporting polypeptides (OATPs), and monocarboxylic acid transporters (MCTs) that are expressed at the BBB and could mediate active transport of statins such as ATV into the brain parenchyma (Wood et al., 2010; Fracassi et al., 2019). In the present study, ATV levels were determined in the cerebral cortex of rats after systemic administration. An average brain:plasma ratio of 0.41 was determined at 1 h after administration, indicating that 40 % of the plasma level of ATV penetrates into the brain. A similar percentage of BBB penetration of the highly lipophilic ATV was reported by an in vitro study, using a human BBB model (Lübtow et al., 2020). Furthermore, among various statins, ATV is the statin most commonly reported effective in preclinical rodent model studies of antiepileptogenesis, and has the most statistically significant association with epilepsy risk reduction in retrospective clinical studies (Hufthy et al., 2022), which would indicate that ATV penetrates into the human brain.

As described above, CTX alone modifies but does not prevent PTE in the FPI rat model used here (Goodrich et al., 2013). Similarly, LEV or ATV alone do not prevent epilepsy in rodent models but have been reported to exert disease-modifying effects in models of epileptogenesis, including kindling (Scicchitano et al., 2015; Klein et al., 2020; Löscher, 2020; Schidlitzki et al., 2020). Thus, the antiepileptogenic effect of TC-002 observed in two different models of acquired epilepsy in two different species (Welzel et al., 2021; present study) is most likely a result of the drug-drug interactions on epileptogenic brain targets illustrated in Table S2.

Regarding TC-001, the only difference to TC-002 is that TPM was used instead of CTX. As noted, a combination of LEV and TPM partially prevented epilepsy in the IHK mouse model (Schidlitzki et al., 2020), while LEV alone was ineffective and TPM alone was less effective than the combination (Löscher and Klein, 2022). ATV was added to the combination of LEV and TPM tested previously in mice (Schidlitzki et al., 2020) because statins such as ATV exert antiinflammatory and neuroprotective effects (Scicchitano et al., 2015) and are the only drugs with clinical antiepileptogenic efficacy in large randomized controlled studies (Klein et al., 2020; Hufthy et al., 2022). Although these clinical trials were performed in stroke patients, we thought that the antiepileptogenic efficacy of ATV suggested by these trials would enhance the efficacy of the LEV plus TPM combination. Furthermore, ATV was also a component of the triple combination TC-002. As shown in Table S2, the drugs (LEV, TPM, ATV) combined in TC-002 interfere with several mechanisms thought to be critically involved in epileptogenesis (Table S2) but TC-001 did not exert any significant antiepileptogenic effect in the rat FPI model here. However, in contrast to the lower dose of TC-002, no mouse:rat allometric dose scaling was used for the rat experiment with TC-001. As shown for TC-002 here and in our previous mouse experiments (Welzel et al., 2021), the dose level seems to be critical for the antiepileptogenic effect of a drug combination in rodent models of acquired epilepsy. This is an important finding because preclinical experiments on antiepileptogenic drug effects are typically only performed at one dose level, which may lead to false negative effects

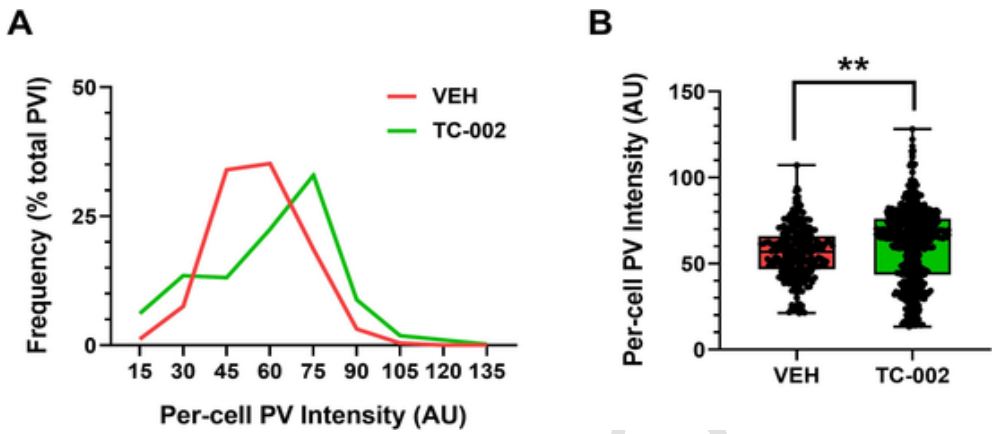

Fig. 11. The effect of TC-002 (LEV, ATV, CTX) on the parvalbumin (PV) expression per PV-positive interneuron (PVI). (A) Frequency distribution of per-PVI PV pixel intensity in perilesional cortex 12 weeks after TBI in FPI-vehicle and FPI-TC-002 rats. (B) Significant increase in mean PV content per PV-positive cell in FPI-TC rats vs. FPI-vehicle controls. Data are shown as boxplots with whiskers from minimum to maximal values; the horizontal line in the boxes represents the median value. In addition, individual data are shown; **p < 0.01.

(Löscher and Brandt, 2010; Löscher, 2020; Dulla and Pitkänen, 2021). One of the few exceptions is a study by Suchomelova et al. (2006) in the lithium-pilocarpine rat model, in which TPM administered at a dose of 10 mg/kg after SE prevented the development of epilepsy whereas TPM was ineffective at 50 mg/kg.

For drug combinations as tested here, the dose dependency of an antiepileptogenic effect is even more complicated when assuming synergistic drug-drug interactions on brain protein networks as suggested by the in silico STITCH analysis illustrated in Fig. S3. Doses for an optimal synergistic drug-drug interaction may be orders of magnitude below doses by which each drug acts when administered alone (Ainsworth, 2011). Thus, ideally, various doses and dose ratios should be tested for antiepileptogenic efficacy of a rationally chosen drug combination, which, however, is not possible in laborious in vivo rodent models of PTE. For the latter purpose, in vitro organic hippocampal slice culture models of PTE (Dzhala and Staley, 2015) or the recently developed PTE zebrafish model (Cho et al., 2020) may allow prescreening of drug combinations before subsequent testing in a rodent PTE model.

Only a few previous studies reported antiepileptogenic drug effects in rodent models of PTE, whereas most previous studies using single drug treatment were negative (Dulla and Pitkänen, 2021). In the controlled cortical impact (CCI) model of PTE in CD1 mice, Guo et al. (2013) reported a reduced incidence of epilepsy following post-injury treatment with the mTOR inhibitor rapamycin. In the lateral FPI rat model, Campbell et al. (2014) reported a reduction of spontaneous non-convulsive seizures following post-injury treatment with the calcineurin inhibitor tacrolimus. A study with the protein phosphatase 2 A activator sodium selenate in the lateral FPI rat model failed to reduce the incidence of PTE but reported a reduced frequency and duration of spontaneous seizures, i.e., a disease-modifying effect (Liu et al., 2016). We previously reported a pronounced antiepileptogenic effect of focal cooling in the FPI rat model (D'Ambrosio et al., 2013).

There has been a previous debate as to whether the short spontaneous recurrent epileptiform ECoG events (EEEs) reported in the weeks and months following FPI in the present version of this model represent seizures or normal electrical activity, which may occur more often after brain injury (D'Ambrosio et al., 2009; D'Ambrosio and Miller, 2010a; D'Ambrosio and Miller, 2010b; Dudek and Bertram, 2010; Rodgers et al., 2015; Bragin et al., 2016; Reid et al., 2016; Smith et al., 2018). As reported previously (D'Ambrosio et al., 2004; D'Ambrosio et al., 2005; D'Ambrosio and Miller, 2010a, 2010b), the EEEs, which were not observed in age-matched sham-injured rats, exhibited evolution in amplitude and waveform, but no obvious postictal suppression (ECoG "flattening") was observed (Fig. 2B-D and Fig. 8A). However, absent postictal suppression does not argue against this being focal seizures because not all focal seizures are followed by postictal suppression (Fisher et al., 2014). For instance, in an analysis of postictal suppression in patients with focal-onset seizures, short focal seizures showed no postictal suppression in the intracranial EEG (Payne et al., 2018). We note also that although postictal ECoG slowing may be difficult to detect by visual inspection, spectral ECoG analysis shows that the spontaneous EEEs after FPI (independent of duration), were immediately followed by an ECoG slowing as is consistent with a postictal state as occurring after seizures (D'Ambrosio et al., 2009). In contrast, random ECoG events in rats were not followed by ECoG slowing. Furthermore, as described previously by D'Ambrosio et al. (2009) and others (Bragin et al., 2016; Reid et al., 2016), further indicating that the paroxysmal EEEs reflect focal seizures, all EEEs lasting ≥1 s were accompanied by behavioral changes that typically consisted of a movement arrest ("freezing") with or without facial automatisms, or, less often, a stereotyped loss of posture at times with motor manifestations such as facial automatisms. Similar behavioral alterations associated with EEG seizure signatures have been characterized as focal (limbic) seizures in several other models of acquired focal epilepsies (Curia et al., 2008; Fisher et al., 2014; Rusina et al., 2021; Löscher and White, 2023). As in these other models, repetitive high-frequency oscillations were recorded from microelectrodes in cortical areas within or adjacent to the TBI core early after FPI (before the onset of focal seizures) but never in sham-injured controls, supporting the use of the FPI rat model as a model for PTE (Bragin et al., 2016; Reid et al., 2016).

The present study has several limitations. First, as previously reported (D'Ambrosio et al., 2009; Bragin et al., 2016; Reid et al., 2016).), in the early months post-injury, the predominant seizure type in the FPI model used here are relatively short ECoG nonconvulsive seizures that are never observed in sham-injured animals, whereas convulsive seizures are rarely observed up to 3 months after FPI. The group of David Poulsen has described a severe version of the lateral FPI model in adult male Wistar rats in which up to 63 % of rats experienced at least one convulsive seizure within 2–5 weeks after FPI (Smith et al., 2018). We tried to reproduce this model but failed (Mustafa Hameed and Alexander Rotenberg, unpublished data). In human PTE patients, both clinic-electrographic seizures and EEG seizures only (subclinical seizures) are commonly observed, the latter similar to the rat ECoG seizures reported here (D'Ambrosio et al., 2009).

Second, as reported by D'Ambrosio et al. (2009) and also observed here, the EEG discharges recorded in the FPI model are accompanied by behavioral alterations that qualify as electroclinical seizures regardless of their duration (Fisher et al., 2014). However, because most of the behavioral alterations observed during the EEG discharges are subtle and best recorded by direct observation of the rats, a reliable post hoc analysis in the videos of the video-EEG monitoring periods is difficult and associated with errors. Thus, we did not separately analyze the behavioral seizures, which is a limitation.

Third, the sample size of the pilot experiments with TC-002 was small. However, the pronounced antiepileptogenic effect observed with the reduced dose of TC-002 was substantiated by the neuroprotective activity of this drug combination. Furthermore, the present findings with TC-002 in the rat FPI/PTE model replicate the previous findings of Welzel et al. (2021) in the intrahippocampal kainate mouse model in another epilepsy model and another species. We plan to replicate the favorable effect of TC-002 observed in the rat FPI model of PTE here in the CCI mouse model of PTE.

Fourth, experiments using TC-001 were performed at the University of Washington, while those using TC-002 were performed at Boston Children's Hospital, which, although unlikely, could lead to unknown differences between these two sites that could account for different outcomes. Furthermore, FPI was performed differently between the two sites (left vs right hemispheres) and different types of EEG monitoring (tethered vs. telemetric) were used, which, however, are unlikely to affect the outcome of treatments.

Fifth, as described in Methods and section 3.2, the two experiments with TC-002 not only differed concerning drug doses but also several other experimental factors that could contribute to the marked difference in the outcome of treatment.

In conclusion, based on a systematic evaluation of various rationally chosen drug combinations in the IHK mouse model performed over the last 12 years (Löscher and Klein, 2022), we have identified a combination of LEV, ATV, and CTX that prevents epilepsy in two rodent models (post-SE and post-FPI) of acquired epilepsy in two species (mice and rats). As shown by testing different doses of TC-002 in both models, the dosing of the drug combination was critical to achieve an antiepileptogenic effect, which may be related to CTX's negative effect on GABAergic inhibition at high doses. The antiepileptogenic and neuroprotective effects of TC-002 in a rat PTE model reported here occurred at plasma and brain levels that were previously reported for humans, thus substantiating that drug level determinations are essential to judge whether preclinical effects occur at relevant drug concentrations in the plasma and brain. Furthermore, such information is critical to allow extrapolation from animal studies to human study design (Klein et al., 2020). In the translation of our results to clinical trials, the dose-dependent pro- versus anti-epileptogenic effects of TC-002 will need to be addressed.

CRediT authorship contribution statement

Mustafa Q. Hameed: Writing – review & editing, Writing – original draft, Visualization, Software, Methodology, Investigation, Formal analysis, Conceptualization. **Raimondo D'Ambrosio:** Writing – review & editing, Visualization, Software, Methodology, Investigation, Formal analysis, Conceptualization. **Cliff Eastman:** Writing – review & editing, Visualization, Software, Methodology, Investigation, Formal analysis, Conceptualization. **Benjamin Hui:** Methodology, Investigation. **Rui Lin:** Methodology, Investigation. **Sheryl Anne D. Vermudez:** Methodology, Investigation. **Amanda Liebhardt:** Methodology, Investigation. **Yongho Choe:** Methodology, Investigation. **Pavel Klein:** Writing – review & editing, Project administration, Funding acquisition. **Chris Rundfeldt:** Writing – review & editing, Project administration, Funding acquisition. **Wolfgang Löscher:** Writing – review & editing, Writing – original draft, Funding acquisition, Conceptualization. **Alexander Rotenberg:** Writing – review & editing, Supervision, Resources, Project administration, Methodology, Funding acquisition, Conceptualization.

Uncited reference

Wen et al., 2018

Declaration of competing interest

PK, CR, WL, and AR are co-founders and have equity in PrevEp Inc., Bethesda, MD. The other authors declare no conflict of interest.

Acknowledgments

The experiments were supported by a grant (1R43NS119081-01A1) to PrevEp and Boston Children's Hospital from the National Institute of Neuronal Disorders and Stroke (NINDS) of the US National Institutes of Health (NIH).

Data availability

Data will be made available on request.

Appendix A. Supplementary data

Supplementary data to this article can be found online at https://doi.org/10.1016/j.expneurol.2024.114962.

References

Ainsworth, C., 2011. Networking for new drugs. Nat. Med. 17, 1166–1168.
Amakhin, D.V., Soboleva, E.B., Zaitsev, A.V., 2018. Cephalosporin antibiotics are weak blockers of GABAa receptor-mediated synaptic transmission in rat brain slices. Biochem. Biophys. Res. Commun. 499, 868–874.
Antwi, P., Atac, E., Ryu, J.H., Arencibia, C.A., Tomatsu, S., Saleem, N., Wu, J., Crowley, M.J., Banz, B., Vaca, F.E., Krestel, H., Blumenfeld, H., 2019. Driving status of patients with generalized spike-wave on EEG but no clinical seizures. Epilepsy Behav. 92, 5–13.
Bragin, A., Li, L., Almajano, J., Alvarado-Rojas, C., Reid, A.Y., Staba, R.J., Engel, Jr, J., 2016. Pathologic electrographic changes after experimental traumatic brain injury. Epilepsia 57, 735–745.
Butler, T., Ichise, M., Teich, A.F., Gerard, E., Osborne, J., French, J., Devinsky, O., Kuzniecky, R., Gilliam, F., Pervez, F., Provenzano, F., Goldsmith, S., Vallabhajosula, S., Stern, E., Silbersweig, D., 2013. Imaging inflammation in a patient with epilepsy due to focal cortical dysplasia. J. Neuroimaging 23, 129–131.
Cabungcal, J.H., Steullet, P., Kraftsik, R., Cuenod, M., Do, K.Q., 2013. Early-life insults impair parvalbumin interneurons via oxidative stress: reversal by N-acetylcysteine. Biol. Psychiatry 73, 574–582.
Cammarota, M., Losi, G., Chiavegato, A., Zonta, M., Carmignoto, G., 2013. Fast spiking interneuron control of seizure propagation in a cortical slice model of focal epilepsy. J. Physiol. 591, 807–822.
Campbell, J.N., Gandhi, A., Singh, B., Churn, S.B., 2014. Traumatic brain injury causes a tacrolimus-sensitive increase in non-convulsive seizures in a rat model of post-traumatic epilepsy. Int. J Neurol. Brain Disord. 1, 1–11.
Cantu, D., Walker, K., Andresen, L., Taylor-Weiner, A., Hampton, D., Tesco, G., Dulla, C.G., 2015. Traumatic brain injury increases cortical glutamate network activity by compromising GABAergic control. Cereb. Cortex 25, 2306–2320.
Cho, S.J., Park, E., Telliyan, T., Baker, A., Reid, A.Y., 2020. Zebrafish model of posttraumatic epilepsy. Epilepsia 61, 1774–1785.
Curia, G., Longo, D., Biagini, G., Jones, R.S., Avoli, M., 2008. The pilocarpine model of temporal lobe epilepsy. J. Neurosci. Methods 172, 143–157.
Curia, G., Levitt, M., Fender, J.S., Miller, J.W., Ojemann, J., D'Ambrosio, R., 2011. Impact of injury location and severity on posttraumatic epilepsy in the rat: role of frontal neocortex. Cereb. Cortex 21, 1574–1592.
D'Ambrosio, R., Miller, J.W., 2010a. What is an epileptic seizure? Unifying definitions in clinical practice and animal research to develop novel treatments. Epilepsy Curr. 10, 61–66.
D'Ambrosio, R., Miller, J.W., 2010b. Point. Epilepsy Curr. 10, 90.
D'Ambrosio, R., Fairbanks, J.P., Fender, J.S., Born, D.E., Doyle, D.L., Miller, J.W., 2004. Post-traumatic epilepsy following fluid percussion injury in the rat. Brain 127, 304–314.
D'Ambrosio, R., Fender, J.S., Fairbanks, J.P., Simon, E.A., Born, D.E., Doyle, D.L., Miller, J.W., 2005. Progression from frontal-parietal to mesial-temporal epilepsy after fluid percussion injury in the rat. Brain 128, 174–188.
D'Ambrosio, R., Hakimian, S., Stewart, T., Verley, D.R., Fender, J.S., Eastman, C.L., Sheerin, A.H., Gupta, P., Diaz-Arrastia, R., Ojemann, J., Miller, J.W., 2009. Functional definition of seizure provides new insight into post-traumatic epileptogenesis. Brain

132, 2805–2821.
D'Ambrosio, R., Eastman, C.L., Darvas, F., Fender, J.S., Verley, D.R., Farin, F.M., Wilkerson, H.W., Temkin, N.R., Miller, J.W., Ojemann, J., Rothman, S.M., Smyth, M.D., 2013. Mild passive focal cooling prevents epileptic seizures after head injury in rats. Ann. Neurol. 73, 199–209.
Deshaies, R.J., 2020. Multispecific drugs herald a new era of biopharmaceutical innovation. Nature 580, 329–338.
Devinsky, O., Vezzani, A., O'Brien, T.J., Jette, N., Scheffer, I.E., De Curtis, M., Perucca, P., 2018. Epilepsy. Nat. Rev. Dis. Primers 4, 18024.
Dhamne, S.C., Silverman, J.L., Super, C.E., Lammers, S.H.T., Hameed, M.Q., Modi, M.E., Copping, N.A., Pride, M.C., Smith, D.G., Rotenberg, A., Crawley, J.N., Sahin, M., 2017. Replicable in vivo physiological and behavioral phenotypes of the Shank3B null mutant mouse model of autism. Mol. Autism. 8, 26.
Dhamne, S.C., Modi, M.E., Gray, A., Bonazzi, S., Craig, L., Bainbridge, E., Lalani, L., Super, C.E., Schaeffer, S., Capre, K., Lubicka, D., Liang, G., Burdette, D., McTighe, S.M., Gurnani, S., Vermudez, S.A.D., Curtis, D., Wilson, C.J., Hameed, M.Q., D'Amore, A., Rotenberg, A., Sahin, M., 2023. Seizure reduction in TSC2-mutant mouse model by an mTOR catalytic inhibitor. Ann. Clin. Transl. Neurol. 10, 1790–1801.
Dudek, F.E., Bertram, E.H., 2010. Counterpoint to "what is an epileptic seizure?" by D' Ambrosio and Miller. Epilepsy Curr. 10, 91–94.
Dulla, C.G., Pitkänen, A., 2021. Novel approaches to prevent Epileptogenesis after traumatic brain injury. Neurotherapeutics 18, 1582–1601.
Dzhala, V., Staley, K.J., 2015. Acute and chronic efficacy of bumetanide in an in vitro model of posttraumatic epileptogenesis. CNS Neurosci. Ther. 21, 173–180.
Eastman, C.L., Verley, D.R., Fender, J.S., Stewart, T.H., Nov, E., Curia, G., D'Ambrosio, R., 2011. Antiepileptic and antiepileptogenic performance of carisbamate after head injury in the rat: blind and randomized studies. J. Pharmacol. Exp. Ther. 336, 779–790.
Eastman, C.L., Fender, J.S., Temkin, N.R., D'Ambrosio, R., 2015. Optimized methods for epilepsy therapy development using an etiologically realistic model of focal epilepsy in the rat. Exp. Neurol. 264, 150–162.
Eastman, C.L., Fender, J.S., Klein, P., D'Ambrosio, R., 2021. Therapeutic effects of time-limited treatment with Brivaracetam on posttraumatic epilepsy after fluid percussion injury in the rat. J. Pharmacol. Exp. Ther. 379, 310–323.
Eder, J., Herrling, P.L., 2015. Trends in Modern Drug Discovery. Handb. Exp. Pharmacol. 232, 3–22.
Farahani, H., Norouzi, P., Beheshti, A., Sobhi, H.R., Dinarvand, R., Ganjali, M.R., 2009. Quantitation of atorvastatin in human plasma using directly suspended acceptor droplet in liquid-liquid-liquid microextraction and high-performance liquid chromatography-ultraviolet detection. Talanta 80, 1001–1006.
Fisher, R.S., van Emde, B.W., Blume, W., Elger, C., Genton, P., Lee, P., Engel, Jr, J., 2005. Epileptic seizures and epilepsy: definitions proposed by the international league against epilepsy (ILAE) and the International Bureau for Epilepsy (IBE). Epilepsia 46, 470–472.
Fisher, R.S., Scharfman, H.E., Decurtis, M., 2014. How can we identify ictal and interictal abnormal activity? Adv. Exp. Med. Biol. 813, 3–23.
Fracassi, A., Marangoni, M., Rosso, P., Pallottini, V., Fioramonti, M., Siteni, S., Segatto, M., 2019. Statins and the brain: more than lipid lowering agents? Curr. Neuropharmacol. 17, 59–83.
Godoy, L.D., Prizon, T., Rossignoli, M.T., Leite, J.P., Liberato, J.L., 2022. Parvalbumin role in epilepsy and psychiatric comorbidities: from mechanism to intervention. Front. Integr. Neurosci. 16, 765324.
Guo, D., Zeng, L., Brody, D.L., Wong, M., 2013. Rapamycin attenuates the development of posttraumatic epilepsy in a mouse model of traumatic brain injury. PLoS One 8, e64078.
Hameed, M.Q., Hsieh, T.H., Morales-Quezada, L., Lee, H.H.C., Damar, U., MacMullin, P.C., Hensch, T.K., Rotenberg, A., 2019. Ceftriaxone treatment preserves cortical inhibitory interneuron function via transient salvage of GLT-1 in a rat traumatic brain injury model. Cereb. Cortex 29, 4506–4518.
Hameed, M.Q., Hodgson, N., Lee, H.H.C., Pascual-Leone, A., MacMullin, P.C., Jannati, A., Dhamne, S.C., Hensch, T.K., Rotenberg, A., 2023. N-acetylcysteine treatment mitigates loss of cortical parvalbumin-positive interneuron and perineuronal net integrity resulting from persistent oxidative stress in a rat TBI model. Cereb. Cortex 33, 4070–4084.
Hsieh, T.H., Lee, H.H.C., Hameed, M.Q., Pascual-Leone, A., Hensch, T.K., Rotenberg, A., 2017. Trajectory of Parvalbumin cell impairment and loss of cortical inhibition in traumatic brain injury. Cereb. Cortex 27, 5509–5524.
Hufthy, Y., Bharadwaj, M., Gupta, S., Hussain, D., Joseph, P.J.S., Khan, A., King, J., Lahorgue, P., Jayawardena, O., Rostami-Hochaghan, D., Smith, C., Marson, A., Mirza, N., 2022. Statins as antiepileptogenic drugs: analyzing the evidence and identifying the most promising statin. Epilepsia 63, 1889–1898.
Hughes, J.P., Rees, S., Kalindjian, S.B., Philpott, K.L., 2011. Principles of early drug discovery. Br. J. Pharmacol. 162, 1239–1249.
Ikeda, A., Hirasawa, K., Kinoshita, M., Hitomi, T., Matsumoto, R., Mitsueda, T., Taki, J.Y., Inouch, M., Mikuni, N., Hori, T., Fukuyama, H., Hashimoto, N., Shibasaki, H., Takahashi, R., 2009. Negative motor seizure arising from the negative motor area: is it ictal apraxia? Epilepsia 50, 2072–2084.
Johnson-Anuna, L.N., Eckert, G.P., Keller, J.H., Igbavboa, U., Franke, C., Fechner, T., Schubert-Zsilavecz, M., Karas, M., Müller, W.E., Wood, W.G., 2005. Chronic administration of statins alters multiple gene expression patterns in mouse cerebral cortex. J. Pharmacol. Exp. Ther. 312, 786–793.
Kelly, E., Schaeffer, S.M., Dhamne, S.C., Lipton, J.O., Lindemann, L., Honer, M., Jaeschke, G., Super, C.E., Lammers, S.H., Modi, M.E., Silverman, J.L., Dreier, J.R., Kwiatkowski, D.J., Rotenberg, A., Sahin, M., 2018. mGluR5 modulation of behavioral and epileptic phenotypes in a mouse model of tuberous sclerosis complex. Neuropsychopharmacology 43, 1457–1465.
Kim, K., Lee, S.G., Kegelman, T.P., Su, Z.Z., Das, S.K., Dash, R., Dasgupta, S., Barral, P.M., Hedvat, M., Diaz, P., Reed, J.C., Stebbins, J.L., Pellecchia, M., Sarkar, D., Fisher, P.B., 2011. Role of excitatory amino acid transporter-2 (EAAT2) and glutamate in neurodegeneration: opportunities for developing novel therapeutics. J. Cell. Physiol. 226, 2484–2493.
Klein, P., Tyrlikova, I., 2020. No prevention or cure of epilepsy as yet. Neuropharmacology 168, 107762.
Klein, P., Herr, D., Pearl, P.L., Natale, J., Levine, Z., Nogay, C., Sandoval, F., Trzcinski, S., Atabaki, S.M., Tsuchida, T., van Den, A.J., Soldin, S.J., He, J., McCarter, R., 2012. Results of phase 2 safety and feasibility study of treatment with levetiracetam for prevention of posttraumatic epilepsy. Arch. Neurol. 69, 1290–1295.
Klein, P., Dingledine, R., Aronica, E., Bernard, C., Blümcke, I., Boison, D., Brodie, M.J., Brooks-Kayal, A.R., Engel, Jr, J., Forcelli, P.A., Hirsch, L.J., Kaminski, R.M., Klitgaard, H., Kobow, K., Lowenstein, D.H., Pearl, P.L., Pitkänen, A., Puhakka, N., Rogawski, M.A., Schmidt, D., Sillanpää, M., Sloviter, R.S., Steinhauser, C., Vezzani, A., Walker, M.C., Löscher, W., 2018. Commonalities in epileptogenic processes from different acute brain insults: Do they translate? Epilepsia 59, 37–66.
Klein, P., Friedman, A., Hameed, M., Kaminski, R., Bar-Klein, G., Klitgaard, H., Koepp, M., Jozwiak, S., Prince, D., Rotenberg, A., Vezzani, A., Wong, M., Löscher, W., 2020. Repurposed molecules for antiepileptogenesis: missing an opportunity to prevent epilepsy? Epilepsia 61, 359–386.
Koepp, M., Trinka, E., Löscher, W., Klein, P., 2024. Prevention of epileptogenesis - are we there yet? Curr. Opin. Neurol. . (in press). .
Liu, S.J., Zheng, P., Wright, D.K., Dezsi, G., Braine, E., Nguyen, T., Corcoran, N.M., Johnston, L.A., Hovens, C.M., Mayo, J.N., Hudson, M., Shultz, S.R., Jones, N.C., O' Brien, T.J., 2016. Sodium selenate retards epileptogenesis in acquired epilepsy models reversing changes in protein phosphatase 2A and hyperphosphorylated tau. Brain 139, 1919–1938.
Löscher, W., 2007. The pharmacokinetics of antiepileptic drugs in rats: consequences for maintaining effective drug levels during prolonged drug Administration in rat Models of epilepsy. Epilepsia 48, 1245–1258.
Löscher, W., 2016. Fit for purpose application of currently existing animal models in the discovery of novel epilepsy therapies. Epilepsy Res. 126, 157–184.
Löscher, W., 2020. The holy grail of epilepsy prevention: preclinical approaches to antiepileptogenic treatments. Neuropharmacology 167, 107605.
Löscher, W., Brandt, C., 2010. Prevention or modification of epileptogenesis after brain insults: experimental approaches and translational research. Pharmacol. Rev. 62, 668–700.
Löscher, W., Klein, P., 2021. The pharmacology and clinical efficacy of antiseizure medications: from bromide salts to cenobamate and beyond. CNS Drugs 35, 935–963.
Löscher, W., Klein, P., 2022. New approaches for developing multi-targeted drug combinations for disease modification of complex brain disorders. Does epilepsy prevention become a realistic goal? Pharmacol. Ther. 229, 107934.
Löscher, W., White, H.S., 2023. Animal models of drug-resistant epilepsy as tools for deciphering the cellular and molecular mechanisms of Pharmacoresistance and discovering more effective treatments. Cells 12.
Löscher, W., Klitgaard, H., Twyman, R.E., Schmidt, D., 2013. New avenues for antiepileptic drug discovery and development. Nat. Rev. Drug Discov. 12, 757–776.
Lübtow, M.M., Oerter, S., Quader, S., Jeanclos, E., Cubukova, A., Krafft, M., Haider, M.S., Schulte, C., Meier, L., Rist, M., Sampetrean, O., Kinoh, H., Gohla, A., Kataoka, K., Appelt-Menzel, A., Luxenhofer, R., 2020. In vitro blood-brain barrier permeability and cytotoxicity of an atorvastatin-loaded Nanoformulation against glioblastoma in 2D and 3D models. Mol. Pharm. 17, 1835–1847.
Lucht, F., Dorche, G., Aubert, G., Boissier, C., Bertrand, A.M., Brunon, J., 1990. The penetration of ceftriaxone into human brain tissue. J. Antimicrob. Chemother. 26, 81–86.
MacMullin, P., Hodgson, N., Damar, U., Lee, H.H.C., Hameed, M.Q., Dhamne, S.C., Hyde, D., Conley, G.M., Morriss, N., Qiu, J., Mannix, R., Hensch, T.K., Rotenberg, A., 2020. Increase in seizure susceptibility after repetitive concussion results from oxidative stress, Parvalbumin-positive interneuron dysfunction and biphasic increases in glutamate/GABA ratio. Cereb. Cortex 30, 6108–6120.
Moga, D., Hof, P.R., Vissavajjhala, P., Moran, T.M., Morrison, J.H., 2002. Parvalbumin-containing interneurons in rat hippocampus have an AMPA receptor profile suggestive of vulnerability to excitotoxicity. J. Chem. Neuroanat. 23, 249–253.
Nair, A.B., Jacob, S., 2016. A simple practice guide for dose conversion between animals and human. J. Basic Clin. Pharm. 7, 27–31.
Patsalos, P.N., Berry, D.J., Bourgeois, B.F., Cloyd, J.C., Glauser, T.A., Johannessen, S.I., Leppik, I.E., Tomson, T., Perucca, E., 2008. Antiepileptic drugs--best practice guidelines for therapeutic drug monitoring: a position paper by the subcommission on therapeutic drug monitoring, ILAE Commission on Therapeutic Strategies. Epilepsia 49, 1239–1276.
Payne, D.E., Karoly, P.J., Freestone, D.R., Boston, R., D'Souza, W., Nurse, E., Kuhlmann, L., Cook, M.J., Grayden, D.B., 2018. Postictal suppression and seizure durations: A patient-specific, long-term iEEG analysis. Epilepsia 59, 1027–1036.
Pollock, A.A., Tee, P.E., Patel, I.H., Spicehandler, J., Simberkoff, M.S., Rahal, Jr, J.J., 1982. Pharmacokinetic characteristics of intravenous ceftriaxone in normal adults. Antimicrob. Agents Chemother. 22, 816–823.
Rambeck, B., Jürgens, U.H., May, T.W., Pannek, H.W., Behne, F., Ebner, A., Gorji, A., Straub, H., Speckmann, E.J., Pohlmann-Eden, B., Löscher, W., 2006. Comparison of brain extracellular fluid, brain tissue, cerebrospinal fluid, and serum concentrations of antiepileptic drugs measured intraoperatively in patients with intractable epilepsy. Epilepsia 47, 681–694.
Ravizza, T., Terrone, G., Salamone, A., Frigerio, F., Balosso, S., Antoine, D.J., Vezzani, A., 2018. High mobility group box 1 is a novel pathogenic factor and a mechanistic biomarker for epilepsy. Brain Behav. Immun. 72, 14–21.
Ravizza, T., Scheper, M., Di Sapia, R., Gorter, J., Aronica, E., Vezzani, A., 2024. mTOR and

neuroinflammation in epilepsy: implications for disease progression and treatment. Nat. Rev. Neurosci. 25, 334–350.
Reid, A.Y., Bragin, A., Giza, C.C., Staba, R.J., Engel, Jr, J., 2016. The progression of electrophysiologic abnormalities during epileptogenesis after experimental traumatic brain injury. Epilepsia 57, 1558–1567.
Rodgers, K.M., Dudek, F.E., Barth, D.S., 2015. Progressive, seizure-like, spike-wave discharges are common in both injured and uninjured Sprague-Dawley rats: implications for the fluid percussion injury model of post-traumatic epilepsy. J. Neurosci. 35, 9194–9204.
Rogawski, M.A., Löscher, W., Rho, J.M., 2016. Mechanisms of action of Antiseizure drugs and the ketogenic diet. Cold Spring Harb. Perspect. Med. 6. . pii: a022780.
Ruden, J.B., Dugan, L.L., Konradi, C., 2021. Parvalbumin interneuron vulnerability and brain disorders. Neuropsychopharmacology 46, 279–287.
Rudy, B., Fishell, G., Lee, S., Hjerling-Leffler, J., 2011. Three groups of interneurons account for nearly 100% of neocortical GABAergic neurons. Dev. Neurobiol. 71, 45–61.
Rundfeldt, C., Klein, P., Boison, D., Rotenberg, A., D'Ambrosio, R., Eastman, C., Purnell, B., Murugan, M., Goodkin, H.P., Löscher, W., 2023. Preclinical pharmacokinetics and tolerability of a novel meglumine-based parenteral solution of topiramate and topiramate combinations for treatment of status epilepticus. Epilepsia 64, 888–899.
Rusina, E., Bernard, C., Williamson, A., 2021. The Kainic acid models of temporal lobe epilepsy. eNeuro 8. . ENEURO.0337-20.2021.
Saheki, A., Terasaki, T., Tamai, I., Tsuji, A., 1994. In vivo and in vitro blood-brain barrier transport of 3-hydroxy-3-methylglutaryl coenzyme A (HMG-CoA) reductase inhibitors. Pharm. Res. 11, 305–311.
Schidlitzki, A., Bascunana, P., Srivastava, P.K., Welzel, L., Twele, F., Töllner, K., Käufer, C., Gericke, B., Feleke, R., Meier, M., Polyak, A., Ross, T.L., Gerhauser, I., Bankstahl, J.P., Johnson, M.R., Bankstahl, M., Löscher, W., 2020. Proof-of-concept that network pharmacology is effective to modify development of acquired temporal lobe epilepsy. Neurobiol. Dis. 134, 104664.
Scicchitano, F., Constanti, A., Citraro, R., De Sarro, G., Russo, E., 2015. Statins and epilepsy: preclinical studies, clinical trials and statin-anticonvulsant drug interactions. Curr. Drug Targets 16, 747–756.
Sierra, S., Ramos, M.C., Molina, P., Esteo, C., Vázquez, J.A., Burgos, J.S., 2011. Statins as neuroprotectants: a comparative in vitro study of lipophilicity, blood-brain-barrier penetration, lowering of brain cholesterol, and decrease of neuron cell death. J. Alzheimers Dis. 23, 307–318.
Smith, D., Rau, T., Poulsen, A., MacWilliams, Z., Patterson, D., Kelly, W., Poulsen, D., 2018. Convulsive seizures and EEG spikes after lateral fluid-percussion injury in the rat. Epilepsy Res. 147, 87–94.
Sohal, V.S., Zhang, F., Yizhar, O., Deisseroth, K., 2009. Parvalbumin neurons and gamma rhythms enhance cortical circuit performance. Nature 459, 698–702.
Suchomelova, L., Baldwin, R.A., Kubova, H., Thompson, K.W., Sankar, R., Wasterlain, C.G., 2006. Treatment of experimental status epilepticus in immature rats: dissociation between anticonvulsant and antiepileptogenic effects. Pediatr. Res. 59, 237–243.
Szklarczyk, D., Santos, A., von Mering, C., Jensen, L.J., Bork, P., Kuhn, M., 2016. STITCH 5: augmenting protein-chemical interaction networks with tissue and affinity data. Nucleic Acids Res. 44, D380–D384.
Welzel, L., Bergin, D.H., Schidlitzki, A., Twele, F., Johne, M., Klein, P., Löscher, W., 2021. Systematic evaluation of rationally chosen multitargeted drug combinations: a combination of low doses of levetiracetam, atorvastatin and ceftriaxone exerts antiepileptogenic effects in a mouse model of acquired epilepsy. Neurobiol. Dis. 149, 105227.
Wen, T.H., Binder, D.K., Ethell, I.M., Razak, K.A., 2018. The Perineuronal 'Safety' net? Perineuronal net abnormalities in neurological disorders. Front. Mol. Neurosci. 11, 270.
Wood, W.G., Eckert, G.P., Igbavboa, U., Müller, W.E., 2010. Statins and neuroprotection: a prescription to move the field forward. Ann. N. Y. Acad. Sci. 1199, 69–76.
Yamamoto, T., Rossi, S., Stiefel, M., Doppenberg, E., Zauner, A., Bullock, R., Marmarou, A., 1999. CSF and ECF glutamate concentrations in head injured patients. Acta Neurochir. Suppl. 75, 17–19.
Yimer, E.M., Hishe, H.Z., Tuem, K.B., 2019. Repurposing of the beta-lactam antibiotic, ceftriaxone for neurological disorders: A review. Front. Neurosci. 13, 236.
Zhuang, Z., Shen, Z., Chen, Y., Dai, Z., Zhang, X., Mao, Y., Zhang, B., Zeng, H., Chen, P., Wu, R., 2019. Mapping the changes of glutamate using glutamate chemical exchange saturation transfer (GluCEST) technique in a traumatic brain injury model: A longitudinal pilot study. ACS Chem. Neurosci. 10, 649–657.